UNIVERSIDADE ESTADUAL PAULISTA
"JULIO DE MESQUITA FILHO"
INSTITUTO DE GEOCIÊNCIAS E CIÊNCIAS EXATAS

Trabalho de Formatura

Curso de Graduação em Geologia

WATER MASS RECONSTRUCTION BY Nd ISOTOPIC ANALYSIS FROM MID ATLANTIC OCEANIC SEDIMENTS

Maria Luiza de Carvalho Ferreira

Prof.Dr. Antonio José Ranalli Nardy (orientador)

Prof. Dr. Augusto Mangini (co-orientador)

Rio Claro (SP)
2013

UNIVERSIDADE ESTADUAL PAULISTA
Instituto de Geociências e Ciências Exatas
Câmpus de Rio Claro

MARIA LUIZA DE CARVALHO FERREIRA

WATER MASS RECONSTRUCTION BY Nd ISOTOPIC ANALYSIS FROM MID ATLANTIC OCEANIC SEDIMENTS

Trabalho de Formatura apresentado ao Instituto de Geociências e Ciências Exatas - Câmpus de Rio Claro, da Universidade Estadual Paulista Júlio de Mesquita Filho, para obtenção do grau de Geólogo.

Rio Claro - SP
2013

AGRADECIMENTOS

Eu gostaria de agradecer a instituição Coordenação de Aperfeiçoamento de Pessoal de Nível Superior (CAPES), pela concessão da bolsa de estudos para intercâmbio na Alemanha pelo programa CAPES/DAAD/UNIBRAL. Também aos coordenadores do programa Peter Christian Hackspacher (Unesp Campus Rio Claro) e Ulrich A. Glasmacher (Ruprecht-Karls-Universität Heidelberg).

Gostaria também de agradecer minha família por sempre me permitir focar nos estudos me dando suporte não só financeiro mas também moral, psicológico e amoroso. Em especial a minha mãe que sempre me encheu de carinho e conhecimento.

A minha sala, Geovárzea, que ajudou muito na minha formação profissional e pessoal, dos momentos de provas e trabalhos à momentos descontraídos acompanhadas de conversas geológicas e outras nem tão geológicas assim. Também aos meus companheiros de intercâmbio, Valdivia, Lara, Regiane/Regina, Cabrito, Alemão e Mariana, que fizeram da minha estadia na Alemanha tempos de boas recordações. E também quero dizer um grande obrigada para Eric, que sempre me passou calma, confiança e muitas ajudas com o inglês.

Agradeço ao meu orientador Antonio José Ranalli Nardy por aceitar me orientar em um tema novo para ele e pelo suporte na redação do trabalho. Também ao George Luvizzoto por fazer ser possível a redação do trabalho em inglês e pelo suporte dado durante todo o processo.

I would like to thank you the marine paleoclimatology group from Institut für Umweltphysik (Ruprecht-Karls-Universität Heidelberg) especially Jörg Lippold, Evelyn Böhm, Patrick Blaser and Benny Antz, who gave me all the support into the lab and the development of knowledge into this new study area. Thank you for all patience, theoretical explanations, german “lessons” (sometimes – almost all the time- my german was pretty difficult to understand). I had a really good and scientific experience. Also Augusto Mangini, my co-advisor, first for give me the opportunity which leads me to develop this thesis, second for came to Brazil to participate of my defense and gave me essentials tips and interpretations of the results.

ABSTRACT

Nd isotopic information obtained of Fe-Mn oxyhydroxide coatings marine sediment is used to reconstruct the interplay of water masses in the Mid Atlantic Ocean during the past 22 ka. The method consist of leaching those coatings and measure in Mass Spectrometer to define the εNd values (ε notion that compare the ratio $^{143}Nd/^{144}Nd$ in terms of their deviation from the Chondritic Uniform Resevoir (CHUR) evolution line) correspondent to past bottom sea water. The radiogenic or unradiogenic parameter of waters with Southern and Northern source (SSW and NSW) was captured for the sediments coating and is used to identify their influence in the surrounded area of the studied core at 22 000 years until present. The core is localized in Mid Atlantic Ocean and was collected in the IODP program in site 306 core U1313. The results had presented convinced records, giving evidence that during Holocene deep waters did not experience distinguished changes; the influence of NSW indicating a reduce but not the shutdown of deep water formation in North Atlantic during LGM; and the record data suggest possible contributions of eastern water mass into Mid Atlantic during glacial time.

Keywords: $^{143}Nd/^{144}Nd$. Mid Atlantic Ocean. Deep Sea Waters. Last Glacial Maximum.

RESUMO

Informações isotópicas de Nd obtidas da capa oxidada ferromanganífera de sedimentos marinhos são usadas para reconstruir a interação de massas de água no Oceano Atlântico Médio durante os últimos 22 ka. O método consiste na proxy εNd aplicada nos sedimentos, que consistem em dissolução destes revestimentos com o intuito de isolar o isótopo de Nd, posteriormente medições em espectrômetro de massa são feitas para definir os valores εNd (ε notação que compara ao razão dos isótopos 143Nd/144Nd em termos do seu desvio a partir da linha de evolução do "Chondritic Uniform Resevoir" (CHUR)) correspondentes a porção inferior das águas marinhas do passado. O caráter radioativo ou não radioativo de Águas Originárias do Sul e do Norte (SSW e NSW) foi capturado nestes revestimentos dos sedimentos que são utilizados para identificar a influência destas águas na área em que o testemunho estudado durante 22 000 anos até o presente. O testemunho (IODP site 306 core U1313) está localizado no Oceano Atlântico (porção central) e foi coletado no programa IODP. Os resultados apresentaram registros convincentes, dando evidências de que durante o Holoceno as águas profundas do oceano Atlântico não experimentaram fortes mudanças, também de que a influência de NSW indica uma redução e não uma parada no processo de formação de águas profundas no Atlântico Norte, os dados ainda podem sugerir possíveis contribuições de massas de água provindas da porção leste do oceano na porção central deste durante o período glacial.

Palavras-chave: $^{143}Nd/^{144}Nd$. Oceano Atlântico central. Águas profundas marinhas. Último máximo glacial (LGM).

LIST OF FIGURES

LIST OF TABLES

SUMMARY

1 INTRODUCTION

The study of oceanic circulation within paleoceanography is an important topic to understand the relation of the interplay climate-ocean. The behavior of the oceanic water masses in the past gives valuable information that can be used for hypotheses of future climate changes. Its study is also significant because the oceanic circulation controls the geochemical processes of the ocean basin, the sedimentary patterns and geomorphic features on the ocean floor.

Different proxies have been used to study the distribution of water masses during the different climate changes that have occurred in the history of Earth. These changes from Last Glacial Maximum (LGM) (approximately 24 ka to 19 ka) to the Holocene have been studied manly using proxies based on nutrients ($\delta^{13}C$; Cd/Ca), oxygen isotopes of foraminifera (benthic and planktonic), $\Delta^{14}C$ ventilation ages and ratios of radioactive trace metals (such as $^{231}Pa/^{230}Th$ and Nd) (GUTJAHR et al., 2008). The Nd proxy is a new method increasingly used to reconstruct the past oceanic circulation.

The water masses, their compositions, distributions and mixing have changed during climate changes, however, it is still not well understood if the climate changes influence changes of oceanic circulation or if these changes themselves influence the climate changes.

The most important place of deep water production is in North Atlantic Ocean that generates North Atlantic Deep Water (NADW). It is a composite water mass with North Source Water (NSW) contributions derived from Iceland–Scotland (NEADW) and the Irminger basins (NWADW), Labrador Sea Water (LSW) and Subpolar Mode Water (SPMW). It is suspected that water masses dominated by Southern Source Water (SSW) as Antarctic Bottom Water (AABW) replaced NADW during LGM, replacing NADW to intermediate depths accordingly called Glacial North Atlantic Intermediate Water (GNAIW). However, is not clear when happened the switch to modern circulation patterns (GUTJAHR et al., 2008).

The Nd proxy has been proposed to contribute to these comprehensions (PALMER & ELDERFIELD, 1985; REYNOLDS et al., 1999; VANCE & THIRLWALL, 2002; FRANK, 2002; GUTJAHR et al., 2007; GUTJAHR et al., 2008). The Nd proxy is based on the extracted isotopic signal from Fe-Mn oxyhydroxide coatings from marine sediment cores. Analysis of porewater from marine sediments demonstrate that trace metals (Sr, Nd, Os, Pb, Th) from the sea water column are adsorbed to Fe-Mn oxyhydroxide coatings under oxic to

suboxic conditions (HALEY et al., 2004). Thus, the method of extract trace metals signal from marine sediments corresponds to the signal from deep water masses.

The Nd isotope (radiogenic and unradiogenic) composition of water masses depends on the provenance of continental input. The Nd residence time is 600-2000 years in deep waters, comparable to the water mass mixing time in ocean basin scale (few hundred years). Nd isotopes behave quasi-conservative in ocean water, this provides water masses with distinct isotope compositions. In global ocean scale the average time of oceanic circulation is 1500 years (FRANK 2002), the residence time of Nd in this case becomes a good tracer to reconstruct oceanic circulation.

2 OBJECTIVES

This study has the objective of reconstruct the interplay of South Source Water (SSW) and North Source Water (NSW) in the Mid Atlantic Ocean, related with glacial (LGM) and deglacial episodes into the range from 22 ka to 0 ka. This is examined by measuring εNd values from the core IODP U1313. This area is critical to compare to the three circulation modes theory: 'warm', 'cold' and 'off', (RAHMSTORF, 2002) and to generate data to contribute to the understanding of North Atlantic oceanic circulation switches.

3 LOCALIZATION

The studied core "IODP U1313" (Latitude: 41.0 N, Longitude: -32.95 E, water depth: 3426 m) (Fig. 1) sampled during the international Integrated Ocean Drilling Program (IODP) Leg 306, was obtained from IODP Bremen's core repository. The sampling in Bremen was decided on the base of the age model from (STEIN et al., 2009) and with the aim of studying back to the last 22 000 years.

The core is localized in the northern Atlantic Basin (Fig. 2). The Atlantic Basin extends as S-shaped basin, between the Artic and subantarctic regions, with an area of 94 km2 (KENNETT, 1982). The basin receives a great amount of freshwater discharge from rivers, what generate a high rate of terrigenous sediment.

This basin is the most important place of deep water formation, where NADW is formed in the north, while AABW is formed in the south. This two water masses influence the sedimentation rate and the seawater-sediment interplay in the study core area.

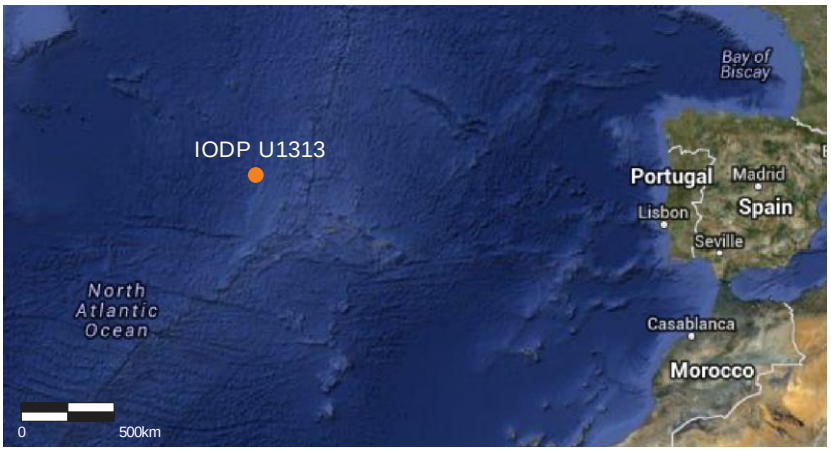

Figure 1(left): Core photo from the first 150 cm revealed from core U1313. Source: http://iodp.tamu.edu/janusweb/imaging/photo.cgi.
Figure 2 (above): Location of the sediment core. Core IODP U1313, situated in North Atlantic ocean, close to Azores island, Latitude: 41.0 N, Longitude: -32.95 E (water depth: 3426 m). Source: google maps.

4 OCEAN CIRCULATION OF THE ATLANTIC OCEAN

Throughout Earth's evolution many changes occurred involving the litho-, bio-, hydro-, cryo- and atmosphere. These systems are closely connected to each other, which means whenever some change occurred in one of them, as consequence it had impact on the other sub-systems. Scientists from interdisciplinary research fields aim to reconstruct past environment, in particular focusing on the last glacial –interglacial cycle.

Several proxies in paleoclimatology have been developed to track and interpret these changes, such as oxygen isotopes ($\delta\ ^{18}O$) as a function of global ice volume (and sea-level) fluctuations and temperature changes, carbon isotopes ($\Delta^{14}C$ and $\delta\ ^{13}C$) to trace deep water masses and Uranium series isotopes (as $^{231}Pa/^{230}Th$) to quantify ventilation rates.

The oceanic circulation, in large scale, is a combination of currents driven by winds (upper hundred meters of the sea), by fluxes of heat and freshwater cross the sea surface given an interior mixing (thermohaline circulation) and tides (gravitacional pull of the Moon and Sun) (RAHMSTORF, 2002).

4.1 Thermohaline circulation

The term thermohaline circulation (as a main driver of the so called Meridional Overturning Circulation) describes the process of water transport due to two factors: temperature and salinity. The increase of salinity and decrease of temperature promote an increase in water masses density, making dense waters sink and less dense waters rise (RAHMSTORF, 2002; BROECKER, 2005; RAHMSTORF, 2006).

A simplification of the thermohaline process is shown in figure 3 displaying the dominance of temperature; surface waters (warm and with higher rates of salinity) flows to higher latitudes (poles) where they lose heat and thus increase in density. These waters sink to the bottom of oceanic basins and form the deep or bottom water masses. As these water masses flows above the oceanic floor, the downward heat diffusion from overlaying masses and geothermal heat cause an increase of their temperature, hence a decrease of density. These waters rise eventually composing intermediate or surface waters (BROECKER, 2005).

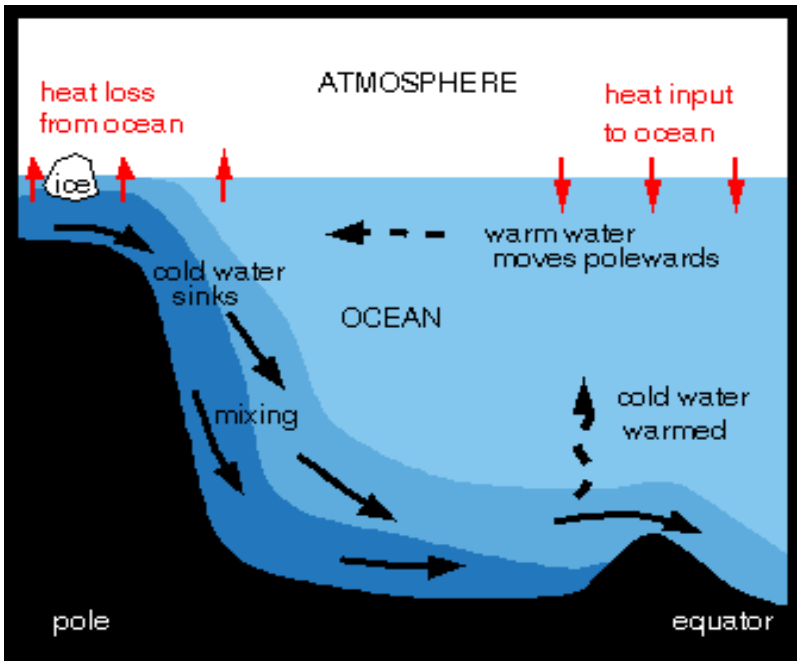

Figure 3: Schematic system of Thermohaline circulation. Surface waters are warmed in equatorial area, transported poleward where they lose heat. Their density is increased and they sink to bottom flowing to lower latitudes. The dense waters are warmed (by heat diffusion) decreasing their density, thus they rise in equatorial areas. Source: http://www.cleanet.org/details/images/28350.html

The Atlantic Ocean exhibits an important piece in the role of ocean circulation and climate, mainly because it is a key place for deep water formation (Fig 4). The sinking of dense waters to the deep (deep water formation) takes place in the high latitudes due to the shallowing of the thermocline.

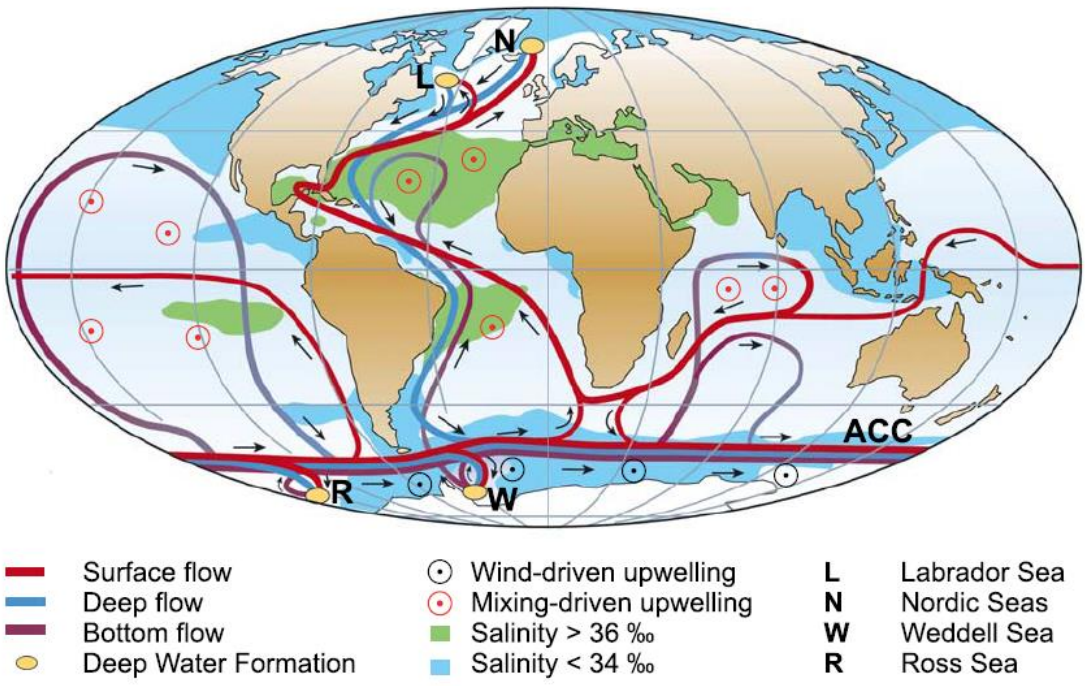

Figure 4: Thermohaline circulation. Source: Kuhlbrodt et al. (2004).

4.2 Present Atlantic circulation

In pole area of North Atlantic Ocean, NADW is formed. It consists mainly of the mixture of three water masses: Iceland Scotland Ridge Overflow Water, Denmark Strait Overflow Water and Labrador Seawater (FRANK 2002). NADW is a fresh water mass with low nutrients content, which flows southward, especially along the Deep Western Boundary Current (DWBC). NADW overlays Antarctic Bottom Water (AABW), owing to its higher density. NADW spreads into most of world's ocean, combines in sub-Antarctic area with circumpolar deep water and rise to Antarctic surface. This water can compose Antarctic Surface Water, Sub-Antarctic Surface Water or Intermediate Surface Water. The Antarctic Surface Water will flow northward to restart the circulation cell (Fig. 5). At the shores of Antarctica surface water lose heat and, mainly, sea ice formation increase it density, therefore it sink to the bottom forming AABW, which is a dense Bottom Water Mass that flows northward.

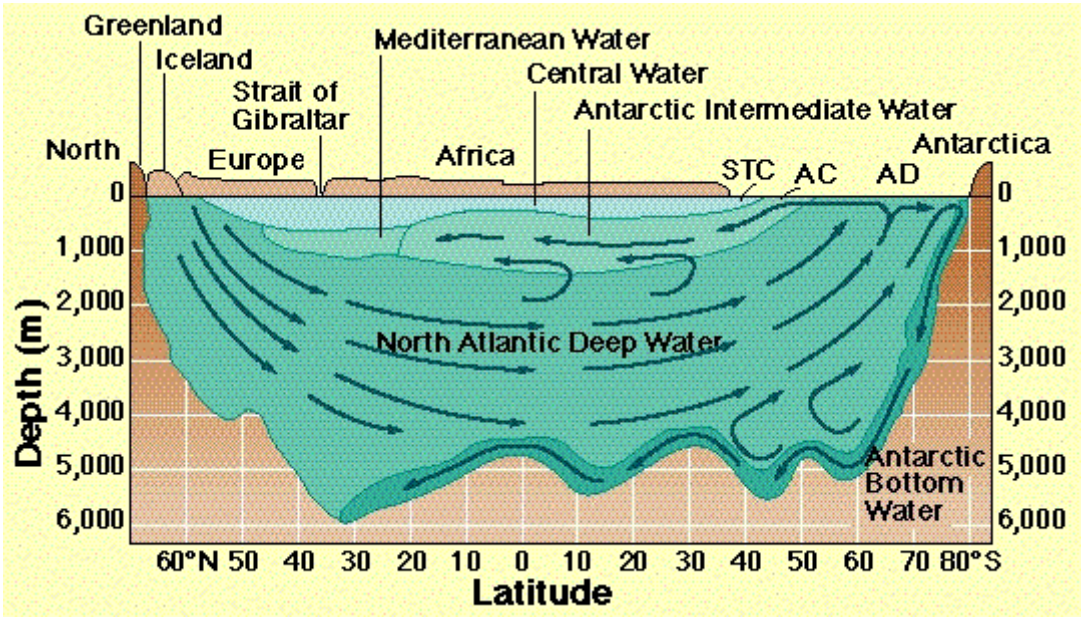

Figure 5: Movements of water masses into the Atlantic Basin. NADW is formed in high northern latitudes and flows southwards, where it starts to mix into intermediate depth. AABW is formed in high southern latitudes and flows northward, where it combines with intermediate waters and flows southward. Source: http://www.geology.wmich.edu/kominz/C9THAtlantic.gif

4.3 Past Atlantic circulation

It is assumed that past circulation during the LGM considerably differed from todays due to the input of fresh water, changed transfer of heat from atmosphere, temperature of atmosphere (and ocean) and the placement of sea ice. It is supposed that the glacial Atlantic Ocean was better stratified (because of the steep salinity and temperature gradients between the water masses) and colder than today.

It is proposed that Glacial NADW did not sink to the very deep, but to the intermediate only. The deep and bottom circulation was dominated by Southern Source Water, that is AABW. It is also proposed that NADW formation was complete interrupted in certain time. Rahmstorf (2002) proposed three distinct modes that show the possible changes in the Atlantic oceanic circulation (Fig. 6). These were labeled as stadial (‘warm’), interstadial (‘cold’) and Heinrich mode (‘off’). While the warm mode represents the modern situation, the cold mode shows that the GNAIW sinks to intermediate depth (about 2.5 km) only and goes to the south. The AABW flows northward until represented an opposing circulation cell. The off mode displays the situation when NADW formation was interrupted, making AABW the water mass responsible for the oceanic circulation.

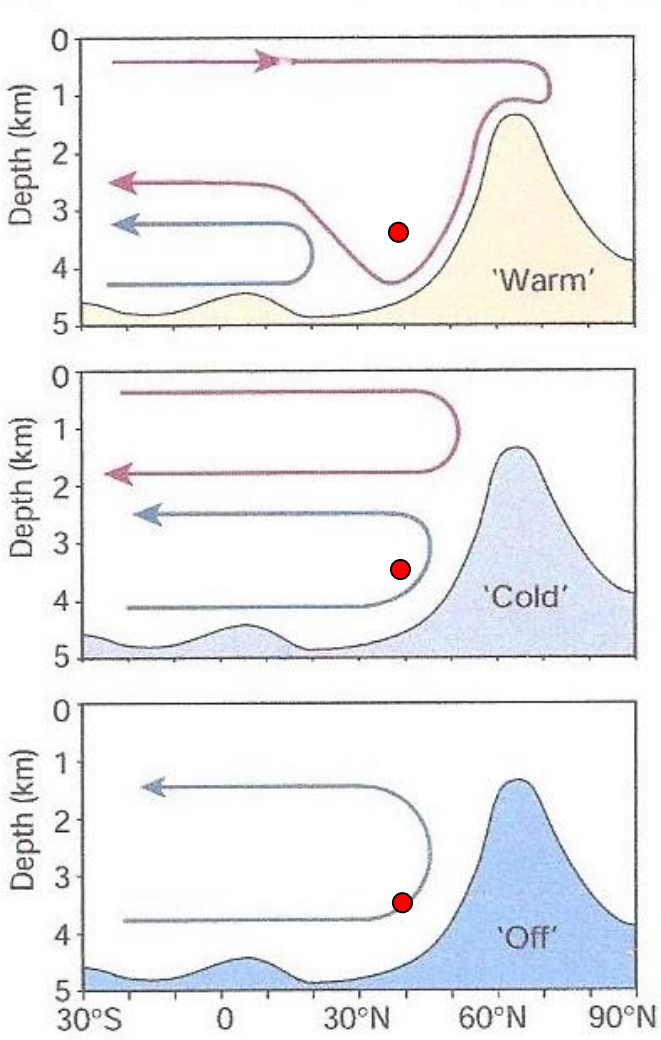

Figure 6: Schematic version of the three modes ('warm', 'cold' and 'off') of ocean circulation as observed during different times of the last glacial period. Shown is the section along the Atlantic, the topographic rise represents the shallow sill between Greenland and Scotland. NADW is highlighted by the red arrow and AABW by the blue arrow. Red dot is the studied sample location. Source: Rahmstorf (2002) (modified).

The studied core is located at latitude 41.0 N, longitude 32.95 E and water depth: 3426 m (represented for the red dots in Fig. 6), and accordingly capable of recording changes potential variations of the influence of Northern or Southern Source Waters as well as their mixing. Since these two water masses have different εNd values, it is possible to identify which of them was mainly responsible for the bottom circulation cell for different time periods.

5 NEODIMIUM PROXY (εNd)

Paleoceanography deals with the development of oceanic basins, such as its currents, shape, salinity and biological productivity. With the knowledge of the oceanic basins behavior is possible to reconstruct past climatic and environmental conditions. Information of paleoceanigraphic reconstruction is stored in sediments. Each proxy has a target, but more

than one proxy can be used to measure the same target. For example to reconstruct the water mass distribution the following proxies can be used: oxygen isotopes of planktonic and benthic foraminifera, nutrients ($\delta^{13}C$, Cd/Ca), water mass $\Delta^{14}C$ ventilations ages, ratios of water-borne radioactive trace metals such as $^{231}Pa/^{230}Th$ and εNd (GUTJAHR et al., 2007). In other words, proxy is a measurable descriptor used to establish a variable (WEFER et al., 1999) represent for εNd and oceanic circulation reconstruction respectively in this study.

The εNd Proxy has been increasingly used to constrain the sources and trace the pathways of water masses. The Nd isotopes (as others trace metals) are incorporated in authigenic Fe-Mn oxyhydroxides coating from marine sediments. Haley et al (2004) studied pore-seawaters and constrained that Fe-oxide and organic matter coatings are the dominant carriers of REEs. Under oxide or sub-oxide conditions, Nd provided from pore-water is trapped in coatings, consequently the bottom seawater Nd isotopes are recorded in sea sediments.

Neodymium (Nd) is a rare earth element, atomic number of 60, average atomic weight of 144.24 (BOWEN, 1988) and has 7 stable isotopes. As all REEs, Nd exists in the 3+ oxidation state and it is found as carbonate ($NdCO_3^+$) or as sulphate ($NdSO_4^+$) complex. Its removal from water column is by particulate scavenging (adsorption) process, this explains the low concentration of Nd at the surface and the desorption/disaggregation process explains the increase of its concentration with depth. The deposition of Nd in marine and estuarine sediments is the most important sink (FRANK, 2002).

The isotope ^{143}Nd is a decay product of the weakly radioactive isotope ^{147}Sm. The Nd isotopes are represented in epsilon notation (εNd) that compares the isotopic ratio of radiogenic ^{143}Nd and non-radiogenic ^{144}Nd in terms of their deviation from the Chondritic Uniform Resevoir (CHUR) evolution line (equation 1).

$$\varepsilon_{Nd} = \left[\frac{^{143}Nd/^{144}Nd_{sample}}{^{143}Nd/^{144}Nd_{CHUR}} - 1 \right] \times 10^4$$

Equation 1: epsilon notation of Nd isotopes ^{143}Nd and ^{144}Nd. Source: Jacobsen and Wasserburg (1980 apud GUTJAHR et al, 2008).

Assuming that the radiogenic isotope ratios of trace metals are not subject to fractionation induced by biological process or evaporation, the changes in the isotopic composition into water mass can only occur by addition of a different isotopic composition from a reservoir. The addition process is promoted by the release of REE elements from

Earth's crust and input into oceanic basins. The release of Nd is caused mainly by weathering of continental and shelf sediments, and its riverine or eolian input and the subsequent leaching and mobilization from shelf sediments (FRANK, 2002).

5.1 Nd sources and input processes

^{143}Nd is a stable isotope decay product of ^{147}Sm (alpha emission), which decays with a half-life of 106 Gyr, thus the ratio Sm/Nd in rocks and mantle decreases with time. The abundance of ^{143}Nd relative to others non-radiogenic isotopes of Nd (such as ^{144}Nd) in a rock, vary as a function of age and Sm/Nd proportion. The ratio Sm/Nd in Earth's mantle (and mantle-derived rocks) is higher than in crust (and crust-derived rocks), this occurs because Sm stays preferentially in the mantle (FRANK, 2002). This is illustrated in figure 7 that shows the separation of bulk Earth into continental crust and residual mantle. It shows that continental crust has lower $^{143}Nd/^{144}Nd$ ratio, because it is enriched in non-radiogenic Nd isotope, while the residual mantle is enriched in radiogenic Nd isotope and present higher $^{143}Nd/^{144}Nd$ ratio. Comparing both (continental and residual mantle – shown as dashed line in Fig. 7) with the bulk Earth evolution (solid line in Fig. 7) the continental crust present negative while residual mantle positive εNd, this is explain for the same isotopic composition enrichment.

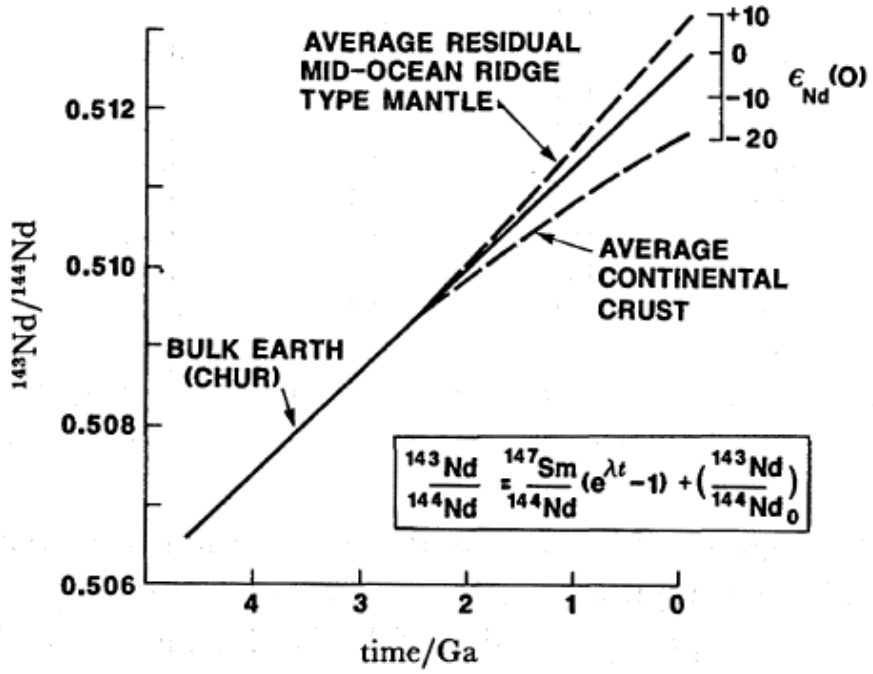

Figure 7: Nd isotope evolution diagram. With the decrease of time the quantity of radiogenic Nd isotope (^{143}Nd) increase in bulk Earth; the residual mantle is enriched in Sm and, consequently, in

radiogenic Nd isotope, while continental crust is enriched in non-radiogenic Nd isotope. In comparison with the curve of bulk Earth the residual mantle has positive values for εNd, because the proportion of radiogenic Nd into it is higher than the bulk average, the opposite happens with continental crust that is enriched in non-radiogenic Nd. Source: Elderfield et al (1988, p. 108).

Using these isotopic compositions of Nd in seawater is possible to identify the sources of Nd. Since each oceanic basin is surrounded by different types and ages rocks, Nd composition in water masses depends on the input of the element in it, thus water masses will present specific εNd values and they are capable of being differentiated. NADW, AABW, and the deep Pacific Ocean have distinct modern neodymium isotopic (εNd) values of approx. -13.5, -8.0 and -4.0, respectively (ELMORE et al, 2011). The difference of εNd values into ocean show the drainage of different Nd sources, for example the North Atlantic is surrounded for continental Proterozoic or Archean rocks which provide εNd values around -40; in contrast, Pacific is surrounded by island arc rocks, which provide εNd values around +20 (FRANK, 2002).

The main sources of Nd in ocean water (Fig 8) are continental sediments (formed by the process of weathering) and volcanic dust by winds (eolian). As shown by Tachikawa et al. (1999) the eolian transport plays an important role in the Atlantic Ocean. As well as the input by rivers and the release of Nd by leaching and mobilization from the continental slope. The hydrothermal process does not show significant contribution to the Nd input, due to the precipitation of Nd within or very close to the hydrothermal sources (FRANK, 2002).

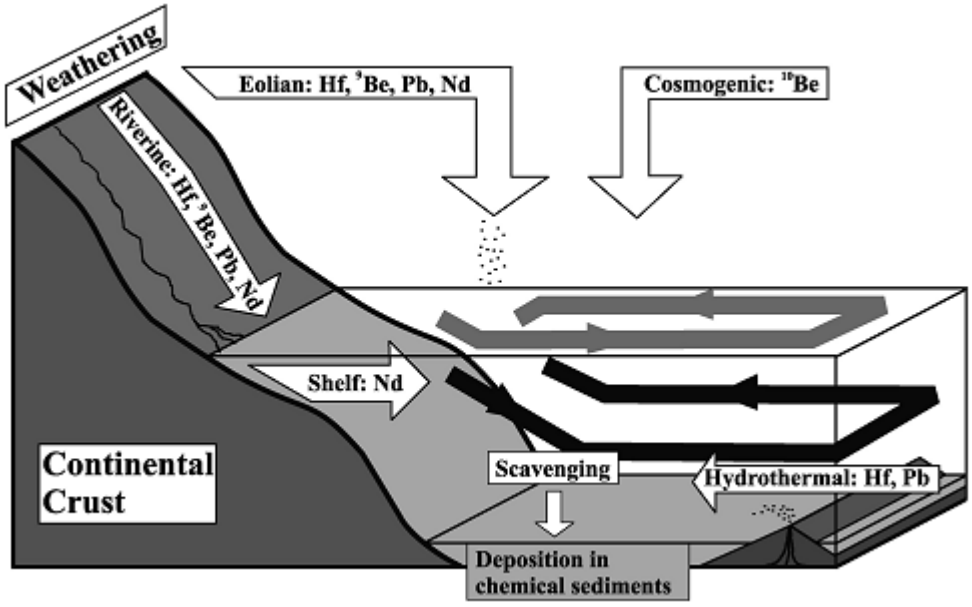

Figure 8: Pathways of trace metals from their sources to their sinks. Nd has basically three soucers: riverine, eolian and shelf. The weathering releases continental sediments that contain Nd, they are transported by rivers and wind (vulcanic ashes also can be tranported by wind). Partial dissolution of shelf sediments also release Nd into seawater. The circulation processes (shown as grey and black

arrows) causes mixing of the trace metals, which are deposited by scavenging process. Source: Frank (2002).

5.2 Removal of REE (Nd) from sea water

In order to reconstruct past oceanic circulation, trace metals with shorter residence time than the average circulation time of the global ocean (1500 years) are used. This is important because if the trace metal has a very short residence time (for example Th 5-20 years), the water mass will not be able to produce a typical signature. The opposite happen with the ones with too long residence times (for example Sr 2-4 Myr), their isotopic composition in water mass will be constant through time. As well the half-time of a radioactive trace metal has also to be longer than the oceanic mixing times (FRANK, 2002; BAYON et al, 2002, GUTJAHR et al., 2008).

These requirements are fulfilled by Nd for this aim, which has a residence time of 600-2000 years (Table 1). Because of its short residence time, it is not isotopically homogenized throughout the water masses, therefore is possible to distinguish water masses based on their isotopic signature (PIEPGRAS & WASSERBURG, 1980). Therefore Nd isotopic composition can be used to track the water mass pathways through global circulation and time.

Table 1: Radiogenic Isotope Nd system

Element	*Radiogenic Isotopes*	*Parent Isotopes*	*Half-Life*	*Primordial Isotopes*[a]	*Average Elemental Deep-Water Concentration*	*Average Deep-Water Residence Time, years*	*Input Sources*
Nd	^{143}Nd	^{147}Sm	106 Gyr	^{142}Nd, ^{144}Nd, ^{145}Nd, ^{146}Nd, ^{148}Nd, ^{150}Nd	4 pg g^{-1}	600–2000	erosion of continental crust

Source: Frank (2002)

6 MATERIALS AND METHODS

The εNd method of deriving past bottom water properties from sediment leachates is a new and promising method. The method was provided by the Marine Group led by Prof. A. Mangini and Dr. Jörg Lippold from Institute for Environmental Physics at the University of Heidelberg (Heidelberg, Germany) and supervised by Dr. Jörg Lippold. The sampling was assisted by scientists from Center for Marine Environmental Sciences (MARUM), University of Bremen (Bremen, Germany). The measurements were performed in co-operation with by

Dr. Marucs Gutjahr from the National Oceanography Centre in Southampton (Southampton, United Kingdom) and the GEOMAR Kiel (Kiel, Germany).

6.1 Sampling

The sampling took place in Bremen (Germany) IODP core repository (in 25th January 2013). The core was chosen to provide information about εNd values of bottom seawater from the North Atlantic Ocean during LGM until present. The applied age model used was developed by Stein et al. (2009).

Each sample from the core IODP U1313 was collected with plastic collectors, and subsequently r bagged and labeled. Before starting the chemical procedure, the samples were freeze-dried, afterwards they were powdered and weighted (0,2 g – 0,3 g).

6.2 Nd processing

The method was divided in nine lab steps (Fig. 9), adapted from the protocol described in Gutjahr et al. (2007) and Bayon et al. (2002). Although the chemical and methodical approach is well tested in general, it has to be adapted in order to meet the specific sedimentological requirements of a new core location.

The detailed protocol is included in appendix and the general descriptions are described below.

Loosely absorbed metals were removed using 5 ml 1 M MgCl2 in a shaker for one hour, than centrifuged and rinsed two times with deionised water (Milli-Q system). After 8 ml of a 1M buffer solution (made of HAc and NaAc in a 1:1 ratio, pH 4,66) was used in order to dissolve carbonates on a shaker for three hours, in the middle of the dissolution (after 1h 30 min) the samples were centrifuged (10 min, 4000 rpm) and placed back on the shaker for the resting time. This diluted acid was used for attack the Fe-Mn-oxyhydroxide and not the lattice structures of clay minerals; the centrifuge in the middle of the process was done with the purpose of having a better carbonate dissolution.

After centrifuged the liquid was collected, the Fe-Mn-oxyhydroxide coatings were leached with 8 ml Nd-leach (made of 0.05 M hydroxylamine hydrochloride (HH), 15% distilled acetic acid, 0.03 M Na–EDTA solution, buffered to pH 4 with analytical grade NaOH) for two hours in a shaker. The HH is the reducing agent responsible for the Fe-Mn oxides dissolution, while EDTA prevents the dissolved Nd to readsorb on the remaining

sediments. The sample was centrifuged and 6 ml of leachate were collected with a pipette into beaker. The remaining sample (solid phase after the leaching) was stored.

The succeeding step is the sample's conversion from nitrate to chloride form, thus HNO_3 and HCl are used to remove the organic chemicals. Thereunto the sample was dried, dissolved in 1 ml HNO_3 (concentrate), 1 ml HCl (9 M) + 5 drops H_2O_2 and 3 ml HCl (1 M), drying it between each dissolution for approximately one hour (or until the sample get dry). 1 ml of the liquid was collected for OES measurement, but this measurement will not be discussed in this thesis.

The sample in chloride form is ready to the separation procedure of Nd from the others elements, this procedure was made in two steps (first and second columns). The first column consists of the REE's separation, for this the ion exchange resin "Dowex 50 WX 8" was used. Before start the second column the sample was converted from chloride to nitrate form, drying and dissolved it in 1.2 ml HNO_3 0.05 M.

The second column is responsible for the Nd separation, thereunto the ion exchange resin "LN-Resin mesh 100 μm -150 μm" was used. This final separation is important to separate Nd from others REE that can cause isobaric interference, as the case for Ce, which is more abundant (88.4% of the elemental abundance) in the natural sample than Nd and cause interference at isotopic mass ^{140}Nd (DE LAETER et al., 2003).

The final step is the sample's conversion for the measurement, thereunto it was dissolved in 1.5 ml HNO_3 (0.05 M).

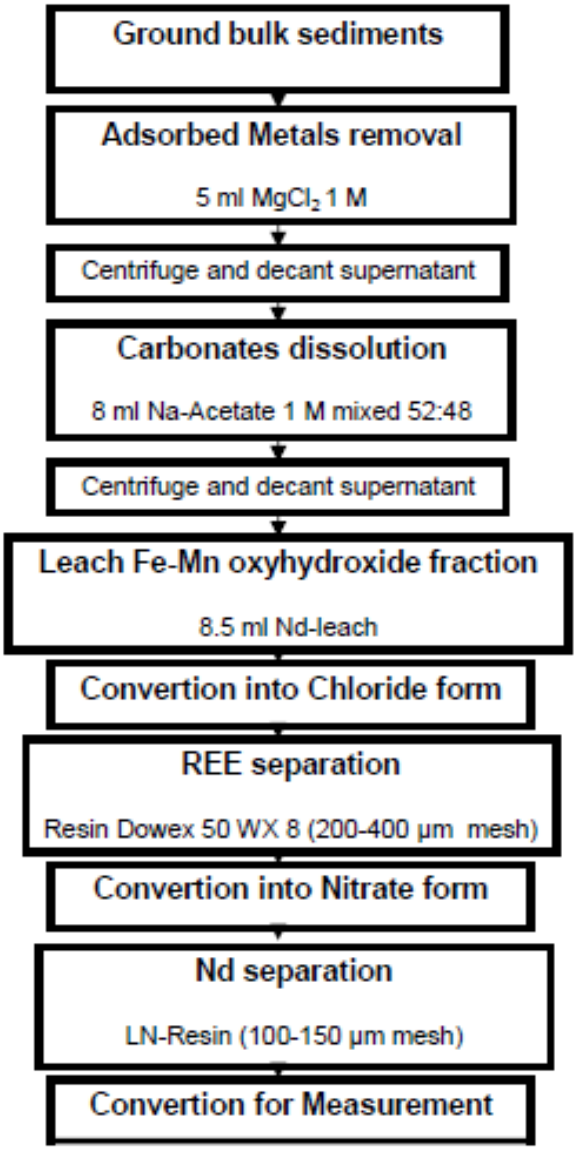

Figure 9: Schematic processing of the Nd separation per sample. Modified from Gutjahr et al. (2007).

6.3 Validations

Gutjahr et al. (2007) describe a 24 hours leaching for guarantee the residual Fe-Mn oxyhydroxide coating complete dissolution, as well as pressure digestion of the detrital sediment fraction. They showed different trace metals concentrations for two hours, 24 hours and detrital dissolution, as well as distinct mid REE enrichment from Fe-Mn oxyhydroxide, while no enrichment is found in detrital fraction. These observations lead to testify the reliability of the method, assuming that the Nd isotopic composition from Fe-Mn oxyhydroxide coating is not from the detritus, but probably from the seawater, and that the leaching procedure of Fe-Mn oxyhydroxide was not contaminated with detritus leaching.

Sr isotopes has been proposed to prove the validation of the method, since it is an element with long residence time in seawater and therefore it displays a homogenous isotopy in the ocean (PALMER & ELDERFIELD, 1985; FRANK, 2002). Thus if the Sr isotopes signal of Fe-Mn oxyhydroxide shows the same value as the seawater signal (range of 0.70917 – 0.70918 87Sr/86Sr, (FRANK, 2002)) it is possible to validate the Sr provenance of seawater. However, Gutjahr et al (2007) showed that even if Sr isotopes from the Fe-Mn oxyhydroxide leachates do not present seawater values still Nd isotopy might be realiable. However, within the scope of this thesis Sr isotopes have not been measured.

6.4 Measurements

6.4.1 Mass Spectrometer (MC-ICPMS)

The mass spectrometer is a machine well used to measure isotopic composition of a wide range of elements, including the heavy radiogenic system as Nd and Sr. It separates atoms or rather ions with a different mass and measure their relative abundance. Its advantage is the versatility, rapidity analysis and mass bias behavior.

The MC-ICPMS determines the mass of a molecule (or element) by measuring the mass-to-charge ratio (m/z) of its ion. First the sample, containing different isotopes of an element, is ionized in inductively coupled plasma (ICP). The ions are accelerated by high voltage and filtered by electric and magnetic fields (perpendicular to the electric field) where the isotopically light and heavy ions are separated because of the Lorentz force (Fig. 10B) and collected (Fig. 10A) (MOOK, 2001). For the calibration different standards can be used, which are defined as isotopic references with a known quantity (ratio) of the target isotopes (TANAKA et al 2000).

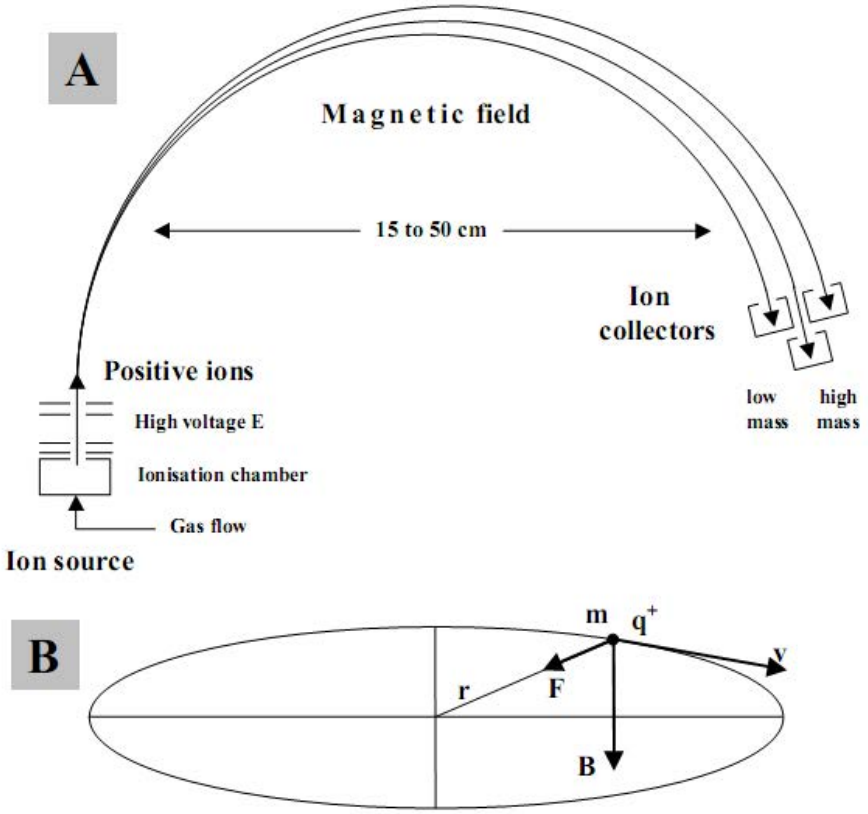

Figure 10: A. Schematic mass spectrometer. The gas passes through the ionization chamber where it is ionized. Its positive ions are accelerated by high voltage E in an electric field. In a magnetic field (perpendicular to the electric field) the ions with a heavier mass follow the larger circle, while the lighter the smaller circle. The ions are colleted and separated into the collectors.
B. Vetorial representation of Lorentz force. A positive electrical particle charged (q+) and mass (m) moves in a flat surface with speed (v), in a magnetic field (B) perpendicular to this surface. The Lorentz force is perpendicular to B and v makes that the particle follows a circular path with radius r. Source: Mook et al. (2001, p. 180).

6.4.2 Measurement procedure

The measurements were made using the Neptune multicollector inductively coupled plasma mass spectrometers (MC-ICPMS) at the National Oceanography Centre, University of Southampton (Southampton, United Kingdom) in November/December 2012; and at the GEOMAR Kiel (Kiel, Germany) in May/2013.

For standard bracketing one JNdi-1 measured for every five samples. The JNdi-1 is neodymium oxide reagent described by Tanaka et al. (2000) that follows two criteria, low abundance of elements that cause isobaric interference (as Ce and Sm) and high $^{143}Nd/^{144}Nd$ ratio. The corrections used were exponential mass bias on $^{146}Nd/^{144}Nd = 0.7219$ and further corrections described in Vance & Thrirlwall (2002).

A Ce-spiked JNdi-1 standard was measured for the mass bias correction. The Ce standard was used because its isobaric interference on ^{142}Nd, for this purpose the ratio $^{142}Ce/^{140}Ce$ was calculated, followed for a secondary mass bias correction (Slope-correction), resulting on a clear ^{142}Nd signal (BLASER, 2013). The compilations of dates and corrections was developed using the software "Microsoft Excel".

7 RESULTS AND DISCUSSIONS

In this chapter the measurement results are present as tables and charts. 46 samples have been fully processed from the core IODP U1313 (Table 2), seven of them were replicated in order to estimate the reproducibility of the measurements. The chart (Fig. 11) of replicate data present results with few deviations, suggesting a good reproducibility of the chemical treatment and measurement.

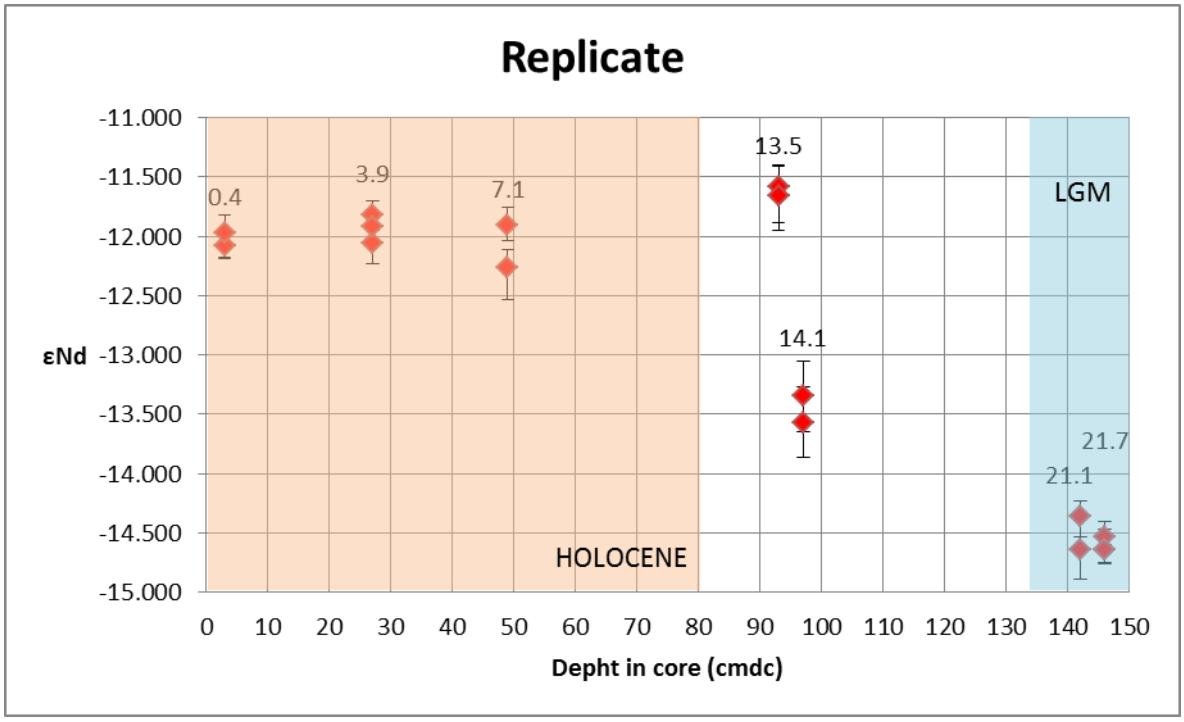

Figure 11: Chart of εNd values and depth in core from the seven replicate samples; light blue area represent LGM period and light pink area represent Holocene. The label above the data refer to the corresponding age (in ka), age model is based on the work by Stein et al (2009).

Table 2: Sample depth (in corrected "meters composite depth" - cmcd), the associated age in kilo years before present (age model from Stein et al 2009), the measured 143Nd/144Nd ratio, εNd values (the epsilon notation that compares the Nd ratio from the sample and the CHUR; CHUR 143Nd/144Nd = 0,51264, Gutjahr et al 2007) and the error (or deviations) from IODP U1313.

Depth [cmcd]	Age [ka BP]	143Nd/144 Nd	εNd	Error in εNd (2σ)
3	0.4	0.51193	-13.853	0.152
3	0.4	0.51194	-13.563	0.151
7	1.0	0.51194	-13.617	0.185
14	2.0	0.51191	-14.234	0.144
21	3.0	0.51191	-14.220	0.190
27	3.9	0.51189	-14.534	0.117
27	3.9	0.51189	-14.642	0.110
27	3.9	0.51190	-14.362	0.067
38	5.5	0.51194	-13.681	0.147
40	5.8	0.51194	-13.543	0.151
42	6.1	0.51194	-13.697	0.155
45	6.5	0.51192	-13.991	0.129
49	7.1	0.51194	-13.567	0.169
49	7.1	0.51195	-13.343	0.253
55	8.0	0.51202	-12.146	0.210
59	8.6	0.51203	-11.815	0.167
62	9.0	0.51199	-12.579	0.238
66	9.6	0.51202	-12.116	0.153
69	10.0	0.51203	-11.893	0.164
73	10.6	0.51206	-11.351	0.160
93	13.5	0.51204	-11.582	0.302
93	13.5	0.51204	-11.655	0.294
94	13.6	0.51201	-12.159	0.096
95	13.8	0.51203	-11.788	0.181
97	14.1	0.51203	-11.905	0.277
97	14.1	0.51201	-12.259	0.127
98	14.2	0.51201	-12.319	0.088
99	14.7	0.51200	-12.488	0.103
101	14.7	0.51205	-11.515	0.181
102	14.8	0.51200	-12.468	0.160
103	15.0	0.51203	-11.810	0.157
107	15.5	0.51201	-12.198	0.150
110	16.0	0.51198	-12.755	0.145
113	16.4	0.51198	-12.863	0.195
115	16.7	0.51196	-13.212	0.203
118	17.1	0.51198	-12.900	0.160
134	19.9	0.51204	-11.624	0.094
135	20.1	0.51205	-11.468	0.138
138	20.6	0.51201	-12.224	0.148
139	20.7	0.51202	-12.146	0.093
140	20.8	0.51201	-12.302	0.092
142	21.1	0.51202	-12.059	0.130
142	21.1	0.51203	-11.916	0.170
145	21.6	0.51200	-12.493	0.074
146	21.7	0.51202	-12.080	0.129
146	21.7	0.51202	-11.974	0.113
146	21.7	0.51203	-11.821	0.199

Figure 12 shows the εNd values (“y” axis) and the coresponding ages (“x” axis). The diamonds represent the measurement datas from Fe-Mn oxyhydroxide coatings fraction of the studied sediment core, which represent variability in the isotopic composition from the deep water mass.

The values can be separated in two trends: higher and lower εNd values. The area which contains higher εNd values is situated before 8 ka until 22 ka, this ages represent the Early Holocene and Upper Pleistocene, during this period the Earth expirienced the last glacial age and the following deglaciation. These values indicate more radiogenic Nd isotopes in the water mass with a relative large range between -13.2 (in 16.7 ka) and -11.3 εNd (in 10. 6 ka) (Fig. 12). In 17 ka the εNd values are the lowest within this time period and they show a continous increase until 14 ka going from -13 to -11.5,.when the values are similar to those found around 9 ka. A similar, however smaller, increase of values are also observed from 22 ka to 20 ka in the order of 0.5 ε units (-12 to -11.5).

The other area contains lower εNd values and represents the more recent ages, from 8 ka until present, totally included by the Holocene. The values are lower owing to the presence of more nonradiogenic Nd isotopes in the water mass situated close to the site. They span a range beteween -14.6 (in 3.9 ka) and -13.3 (in 7.1 ka) (Fig. 12). However the values present a relative stability, is observed that from 6 ka to 4 ka there is the more pronounce decrease of values in order of 1 ε unit. Followed for stable values and the last increase in order of 0.5 ε unit, when the εNd values reach -13.7$\pm$0.1.

The transition from one area to another is marked by an gradual change in the values, with a beginning of εNd values bellow -13. Abrupt changes in εNd do also occur within each specific time period, but it is always (besids one time) eiher below or above -13. Further, two gaps can be observed between 11 ka – 13 ka and 17 ka – 20 ka, owing to the absence of samples selected during these periods. In face of comparison with values found in others studies the present NADW and glacial GNAIW εNd values are discriminated in Figure 11 based on studies by Gutjahr et al. (2008), Roberts et al. (2010), Gutjahr and Lippold (2011). It can be observed that the values from younger ages is in agrrement with the range of present NADW εNd values, in contrast of the older values, which did not reach the full glacial NADW εNd.

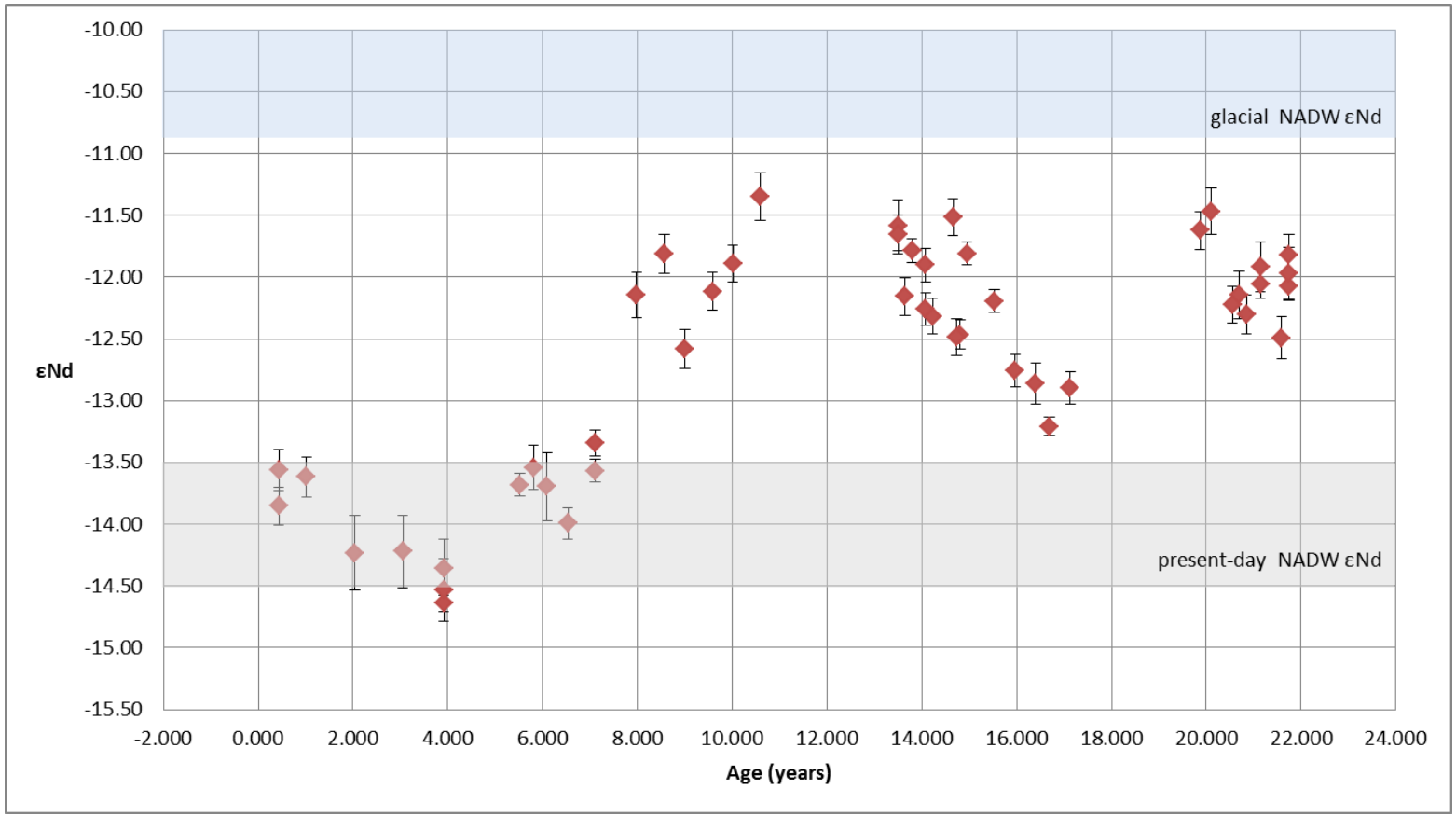

Figure 12: εNd values versus ages of the Site U1313, the measured data are represented by the red diamonds; light grey shaded area represents present-day NADW εNd values; the light blue rectangle represents glacial GNAIW εNd values, both for Northwestern Atlantic extracted from Gutjahr et al. (2008) and Gutjahr and Lippold (2011). The Age model is based on the work by Stein et al. (2009).

The figure 13 shows the interpolated curve of εNd values of the same core. In this chart it is easier to observe the oscillations of the εNd through time. The first increase of values (between 22 ka and 20 ka described above) actually shows brief oscillations until reach the value of -11.5, this event is here associated with LGM. In this period the global ice sheets reached their maximum integrated volume (CLARK et al., 2009).

After this period the values decrease at 17 ka, however, the transition is not well market due to the absence of samples, and could indicate a deep ventilating episode. The second increase (between 16.7 ka and 15 ka) is marked by a continuous rise of 3.3 ε units in approx. 1 ka and could be associated with cooling events and the input of freshwater into the ocean, that could provide a diminishment of deep water formation resulting in more radiogenic εNd. The period between 15 ka and 13.5 ka shows two oscillations in the order of 1 ε unit, at the first the values reach -11.8 while the second -11.6. However, such shifts are roughly the range of reproducibility as marked by the values at 14.7 ka. The maximum εNd value (-11.3) occur at 10.6 ka around the onset of the Holocene preceding the last and more pronounced decrease in the values, which reach values in agreement to present deep water mass values and mark the transition of the last glacial to the present interglacial period. This decrease appears not to be gradually but is interrupted by peaks of higher values, the first in 8.6 ka (-11.8) and one other less pronounced at 5.8 ka (-13.5). Around 4 ka is situated the minimum value (-14.6 εNd), which, in a gradual curve, goes to values reaching -13.7 until recent ages.

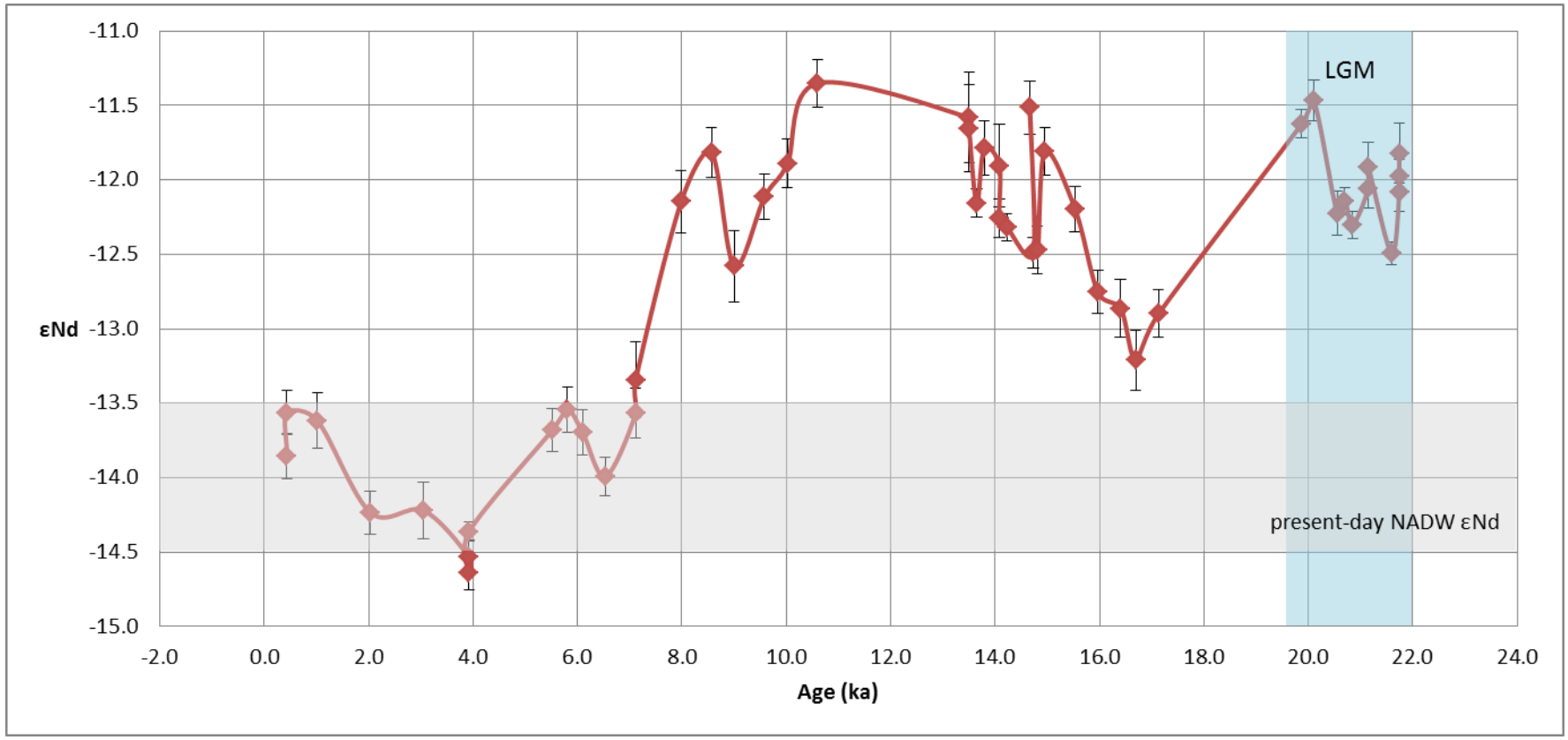

Figure 13: εNd curve, red diamonds represent the measured data; the light blue rectangle represent Last Glacial Maximum; the light gray rectangle represent present-day NADW εNd values for NW Atlantic. The LGM is based on Gutjahr et al. (2008), Gutjahr and Lippold (2011) and interpretation of the studied data record. Age model extracted from Stain et al. (2009).

Some comparisons with results described in the studies by Gutjahr et al. (2008), Roberts et al. (2010) and Gutjahr and Lippold (2011), are here discussed with the aim to compare the correspondence and dissimilarity with the presenting results. This comparison will also be useful to base some considerations of the conclusions.

The data from Roberts et al (2010) and Gutjahr and Lippold (2011) are from the sediment core ODP 1063 situate in the around of Bermuda Rise (western North Atlantic), while the sediment core 12 JPC studied for Gutjahr et al. (2008) is situated along the Blake Ridge (western North Atlantic). The first one is 2 320 km while the second is 3 871 km SW away from the core IODP U1313 (Fig. 14), however both are located within the Western Boundary Undercurrent (WBUC), which transports NADW.

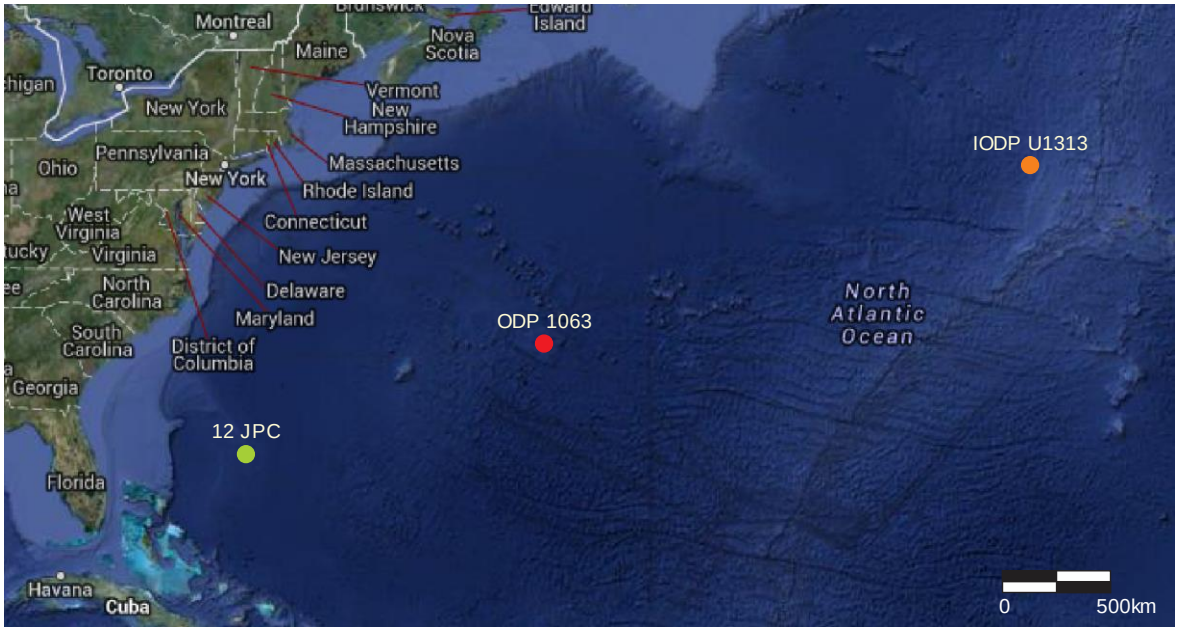

Figure 14 – Map with the cores 12 JPC, ODP 1063 and IODP U1313 locations. Source: google maps.

The figure 15 shows the data from the three authors above cited and the data curve measured in the present study during the past 22 000 years before present. The table of the compiled data and figures extracted directly from the authors studies are presented in annex (ANNEX B).

The first observation is that all of εNd results exhibit some stability and values with more radiogenic Nd isotopes (above -13 εNd) marking the LGM period, which lasts until approx. 18 ka. Although the data values from the present study are generally lower than the others authors. This period is followed for a small and fast decrease in εNd values showed by

Roberts et al. (2010) and Gutjahr et al. (2008) in 17.3 ka and later for the present study in 16.7 ka, which exhibit the lowest εNd values (-13.2).

A continuous increase is observed until approx. 16 ka in all data records, except Gutjahr and Lippold (2011) whom shows an oscillating increase (this could be observed because of the detailed resolution of the sampling). During the period of 16 ka to 14 ka the data exhibit different behaviors.

The following discussions do not consider the Gutjahr and Lippold (2011) study, due their absence of data to more recently ages. In approximately 14.5 ka all of them present a peak with high values which is succeeded by decrease. Gutjahr et al. (2008) show a slow and continuous decrease, while in Roberts et al. (2010) and this study it is abrupt followed for two peaks of more radiogenic Nd isotopes, however the Roberts et al. (2010) data show oscillations more pronounced and greater period of duration. Around 12 ka Roberts et al. (2010) and Gutjahr et al. (2008) founded data in decreasing, marking the Yonger Dryas event (YD); however the presenting data has no record at this period. In both studies values bellow -13 εNd were found after 11.5 ka (end of YD event), other than the present study, on which the values only reach those values in 7 ka. In 9 ka all the tree record show a more unradiogenic Nd values, which in Roberts et al. (2010) and the present study more pronounced. From that date to present the εNd values vary in order of 2 εNd units, remaining within the range -13 and -15 εNd values.

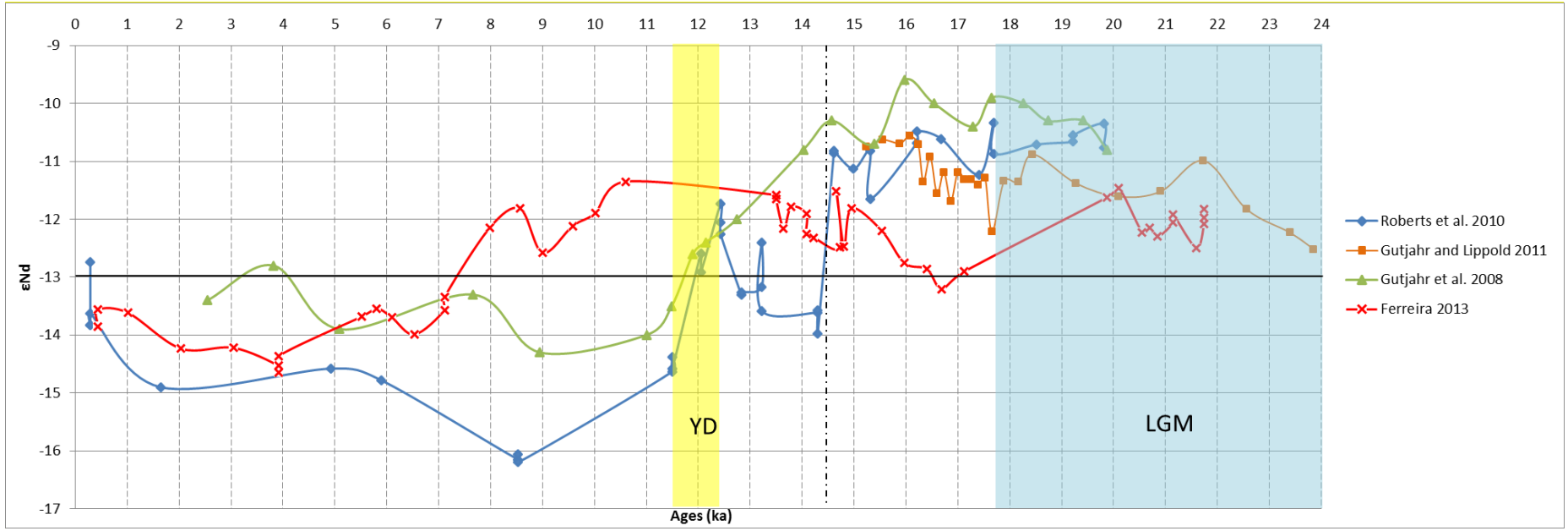

Figure 15 – Chart with εNd values from Gutjahr and Lippold (2011), Roberts et al. (2010), Gutjahr et al. (2008) in comparison with the present study (red curve), measured from sediments core localized into North Atlantic Ocean. See text above to comparisons.

8 CONCLUSIONS

The age model adopted in this study, developed by Stein et al. (2009), is not very robust and can present some shifts (± 2 ka) in concern of it resolution, since it was made by Sea Surface Temperature (Alkenone based) correlated to other cores and is primary made for ages in a large scale (300 ka BP).

The recent data are in agreement with measurement of the NADW, which has εNd value of -13.5 (ROBERTS et al., 2010; FRANK, 2002). This is an evidence to prove that the method of Nd isotopes extraction from Fe-Mn oxyhydroxide is effective and reliable to represent data from water mass.

The stability of εNd values in Holocene suggest that the water mass that circulated this area was not much different from the present NADW, suggesting a northern source of water responsible for the NADW composition and that the deep water formation in North Atlantic was as strong as today. At 4 ka the εNd exhibit lowest εNd values, which can be related to a higher influence of more unradiogenic water masses (NADW), in very good agreement to early/mid Holocene AMOC overshoot, found in several records of paleocirculation e.g. (ROBERTS et al 2010) (see figure in ANNEX C).

According to previous studies (HILLAIRE-MARCEL et al., 2001 apud ROBERTS et al., 2010) the increase of proportion from water mass coming from Labrador Sea into NADW composition occurred approx. 8 ka, this water mass present more unradiogenic εNd and would change the radiogenic signal in NADW, assuming that NADW was a mixture of masses fairly unradiogenic with northern (e.g. water masses coming from Iceland, Greenland and Norwegian with εNd in the range of -7.7 to -10.7) or/and southern source influence (AABW εNd in the range of -7 to -9) (LACAN et al., 2012; GUTJAHR et al., 2008). This could explain the accentuated decrease occurred at 8.6 ka saw in figure 13, which provides the more unradiogenic character to NADW during Holocene. The data record in early Holocene show more radiogenic εNd, which could be related with influence of water masses from southern source (SSW) (Fig 15) with εNd range of -9.4 to -10.1, since the core U1313 is located more eastern than the others core discussed above. It could even suggest that in the same period the oceanic circulation pattern in Mid Atlantic was different that observed in Western Atlantic, since is possible to see, at Early Holocene, the more radiogenic εNd of the samples from IODP U1313 in comparison of ODP 1063 and 12 JPC. The circulation into Mid Atlantic could be related to the “cold” mode from Rahmstorf (2002) (Fig. 6) while in Western

Atlantic the circulation presented the same pattern as present circulation ("warm" mode of Rahmstorf (2002)).

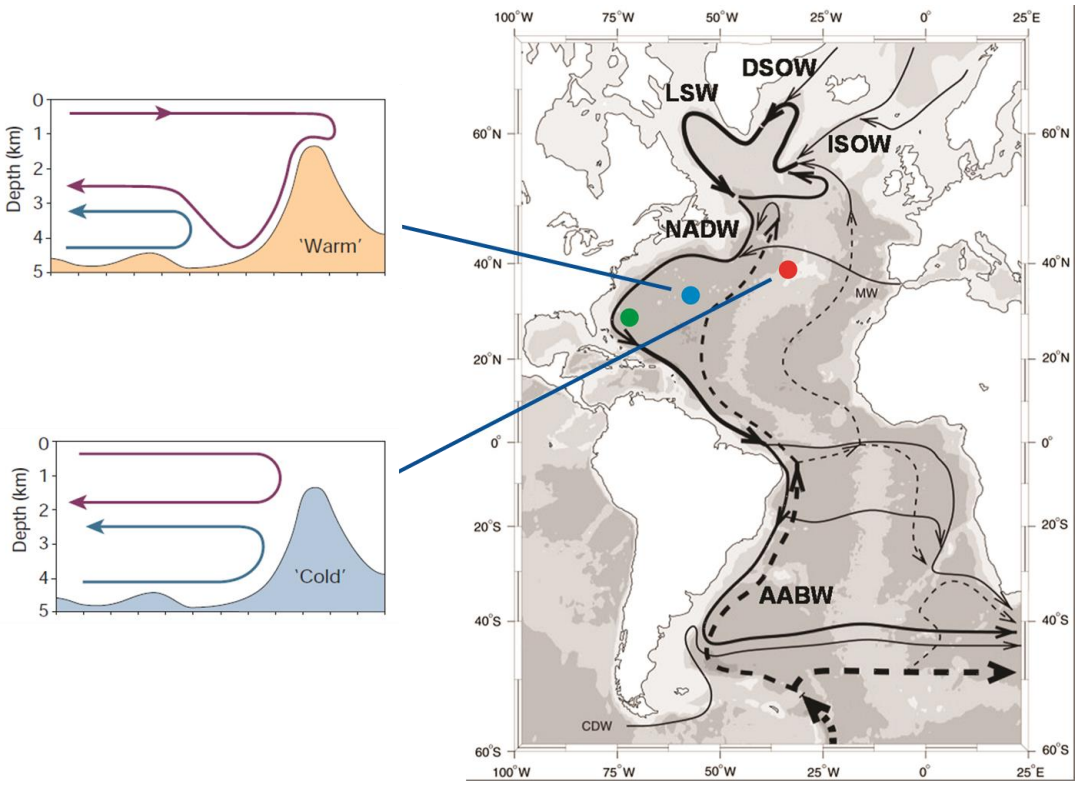

Figure 16 – Representation of the deep waters masses that promotes the deep circulation into Atlantic Ocean. The arrows show the water movement directions. The red dot represent the core IODP U1313, the blue dot the ODP 1063 and the green 12 JPC. The two circulation mode from Rahmstorf (2002). NADW- North Atlantic Deep Water; LSW– Labrador Sea Water; DSOW- Denmark Strait Overflow Water; ISOW- Iceland Scotland Overflow Water; MW- Mediterranean Water; AABW- Antarctic Bottom Water; CDW- Circumpolar Water. Source: Blaser (2013) (modified).

The period that preceding those decrease in εNd values is marked by more radiogenic values. This period is set in the last glacial age. The LGM was determined between 22 ka and 18 ka, when the εNd show radiogenic values, which was associated with the product of radiogenic water masses influence, as SSW and MW. It was observed that those values did not reach the present εNd values from AABW (-7 to -9 εNd), this may suggest that: the AMOC did not shutdown during this period (this was also observed by Gutjahr et al. (2008) and Roberts et al. (2010)), since the GNAIW was not totally influenced by SSW, but also by NSW. However there are still uncertainties in the identity of the water masses that composed the GNAIW and glacial NADW and AABW εNd composition.

The values found in this study show stronger contribution of unradiogenic composition than the data from western Atlantic Ocean (Fig. 15) during and after LGM (before Holocene). Suggesting that the contributions of water masses may not be influence only by NSW and SSW, but also by more unradiogenic masses coming from eastern North

Atlantic (Mediterranean Water) (see table 3 to εNd values of water masses). How the data used to comparison (Fig 15) show more radiogenic pattern, they could be associated with more influence of SSW as well as NSW coming from Iceland, Scotland and Greenland. Suggesting that in past the northern water masses which compose todays NADW had different pathways, although more studies in eastern part of Atlantic (as well as western) should receive attention, leading to understand the shifts in εNd values and water masses circulation.

Climate events such as Heinrich, Yonger Dryas or Dansgaard–Oeschger events (review in Rahmstorf (2002)) could be associated with oscillations observed after LGM. Although more information with different proxies and cores should be consider to propose such correlations.

Table 3: Water masses salinity, εNd values and concentrations with corelated cruise/station and coordinates. LSW: Labrador Sea Water, NEADW; North East Atlantic Deep Water; ISOW: Iceland Scotland Overflow Water; NSDW: Norwegian Sea Deep Water; GSDW: Greenland Sea Deep Water; NACW: North Atlantic Central Water; MW: Mediterranean Water. Source: Lacan et al (2012)

Cruise, station	Depth. (m)	Salinity	ε_{Nd}	2σ	Conc. (pmol/kg)	Water mass
Hudson 83-036 St. 11; 52.08°N -47.02°E	1500	34.872	-14.4	0.4	18.1	LSW
Signature/GINS St. 6; 50.20°N, -45.68°E	1650	34.86	-13.9	0.4	17.4	
Hudson 83-036 St. 11; 52.08°N -47.02°E	2500	34.932	-13.8	0.5	16.7	NEADW
	3000	34.933	-13.4	0.4	17.3	
Signature/GINS St. 6; 50.20°N, -45.68°E	2499	34.90	-13.2	0.4	18.3	
TTO/NAS Station 142; 61.35°N -8.02°E	750	34.905	-7.7	0.6	21.4	ISOW
Signature/GINS St. 23; 60.50°N, -5.00°E	988	34.90	-7.3	0.4	24.6	
TTO/NAS Station 144; 67.67°N -3.28°E	3750	34.909	-9.5	0.5	16.3	NSDW
Signature/GINS St. 26; 69.03°N, 7.95°E	2972	34.90	-9.8	0.4	27.3	
TTO/NAS Station 149; 76.88°N 1.03°E	2800	34.901	-10.7	0.4	16.8	GSDW
Signature/GINS St. 30; 76.74°N, -2.33°E	2512 (unfiltered)	34.90	-10.8	0.4	19.6	
TTO-TAS station 80; 27.83°N, -30°53°E	389	35.942	-11.0	0.8	13.9	NACW
EUMELI Station E3O; 21°N, -31°E	250	36.47	-10.5	0.2	18.6	
	500	35.63	-10.5	0.2	18.2	
Station MED-15; 36.07°N, -6°E	250	-	-9.9	0.5	28.0	MW
	400	38.517	-10.1	0.7	32.4	
Station 5, 35.9°N, -5.65°E	350	38.48	-9.4	0.2	-	

9 OUTLOOK

The present study promoted an insight of Nd isotopic composition of deep waters in North Atlantic during the past 22 ka. The good results were presented in agreement with water measurement records, therefore they contributed to the trustworthiness character of the εNd proxy. The well-established records might be also correlated with the low influence of volcanogenic materials, which promoted in others areas doubtful record (as is seen in cores close to Iceland). Thus, more detailed investigations should be done in this core with the aim to promote reliable information about past oceanic compositions. The use of a different method has a proposition to compare the data record with the coating sediment leachate, for example using fish teeth or foraminifera.

The age model used and developed by Stein et al (2009) is consistence, but it is not very stout, since it was made in large scale (ages > 300 ka) and could present shift in values until $\pm$ 2 ka, which could promote troubling mistakes. To deal with this issue it is necessary to make measurements with ^{14}C.

Besides all the recent emerging data of past ocean and climate changes, many uncertainties still prevail, such as water masses behavior, isotopic composition and oceanic circulations models. This study made some interpretations that could afford with some uncertainties: the reduction but not shutdown of AMOC, stable pattern in Holocene deep waters and more unradiogenic εNd values in Mid North Atlantic Ocean (NAO) than western NAO. Some questions, on the other hand, still surround those contributions, the similarity in isotopic composition of water masses from past and present, mixing processes of water masses, relation between past and present ocean and atmosphere.

References

BAYON, G., GERMAN, C., BOELLA, R., MILTON, J., TAYLOR, R., & NESBITT, R. (2002). An improved method for extracting marine sediment fractions and its application to Sr and Nd isotopic analysis. *Chemical Geology, 187*, 179-199.

BLASER, P. Investigations on the Extraction of Authigenic Neodymium from Marine Sediments. Heidelberg. 2013.

BOWEN, R. (1988). Other Dating Methods. In R. Bowen, *ISOTOPES IN THE EARTH SCIENCES* (pp. 270-283). London and New York: Elsevier Applied Science.

BROECKER, W. S. (2005). *The Role of the Ocean in Climate Yesterday, Today and Tomorrow.* New York: ELDIGIO PRESS.

CLARK, P. U.; DYKE, A. S.; SHAKUN, J. D.; CARLSON, A. E.; CLARK, J.; WOHLFARTH, B.; MITROVICA, J. X.; HOSTETLER, S. W.; MCCABE, A. M. (2009). The Last Glacial Maximum. *Science, 325*, 710-714.

DE LAETER, J. R., BÖHLKE, J. K., DE BIÈVRE, P., HIDAKA, H., PEISER, H. S., ROSMAN, K. J., et al. (2003). Atomic Weights of the Elements: Review 2000 (IUPAC Report). *Pure and Applied Chemistry, 75*, pp. 638-800.

ELDERFIELD, H. (1988). The oceanic chemistry of the rare-earth elements. *Philosophical Transactions*, 105-126.

ELMORE, A. C., PIOTROWSKI, A. M., WRIGHT, J. D., & SCRIVNER, A. E. (2011, September 30). Testing the extraction of past seawater Nd isotopic composition from North Atlantic deep sea sediments and foraminifera. *Geochemistry Geophysic Geosystems, 12*, pp. 1-13.

FRANK, M. (2002, February). Radiogenic isotopes: tracers of past ocean circulation and erosional input. *Reviews of Geophysics, 40*, 1-38.

GUTJAHR, M., FRANK, M., STIRLING, C. H., & V., K. (2007). Reliable extraction of a deepwater trace metal isotope signal from Fe–Mn oxyhydroxide coatings of marine sediments. *Chemical Geology*, 351-370.

GUTJAHR, M., FRANK, M., STIRLING, C. H., KEIGWIN, L. D., & HALLIDAY, A. N. (2008). Tracing the Nd isotope evolution of North Atlantic Deep and Intermediate Waters in the western North Atlantic since the Last Glacial Maximum from Black Ridge sediments. *Earth and Planetary Science Letters 266*, 61-77.

GUTJAHR, M. & LIPPOLD, J. (2011). Early arrival of Southern Source Water in the deep North Atlantic prior to Heinrich event 2. *Paleoceanography 26.*

HALEY, B. K. (2004). Rare earth elements in pore waters of marine sediments. *Geochimica et Cosmochimica, Acta 68 (6)*, 1265–1279.

KENNETT, J. P. (1982). *Marine Geology.* New Jersey: Prentice-Hall.

KUHLBRODT, T., GRIESEL, A., MONTOYA, M., LEVERMANN, A., HOFMANN, M., & RAHMSTORF, S. (2004). On the driving process of the Atlantic Meridional Overturning Circulation. *Reviews of Geophysics, 45*, 1 - 32.

LACAN, F., TACHIKAWA, K., & JEANDEL, C. (2012). Neodymium isotopic composition of the oceans: A compilation of seawater data. Chemical Geology, 300, 177-184.

MOOK, W., GAT, J., MEIJER, H., ROZANSKI, K., & FROEHLICH, K. (2001). *Environmental isotopes in the hydrological cycle: principles and applications* (Vols. 1 - Introduction: Theory, Methos, Review).

PALMER, M. R., & ELDERFIELD, H. (1985). Variations in the Nd isotopic composition of foraminifera from Atlantic Ocean sediments. *Earth and Planetary Science Letters, 73*, 299-305.

PIEPGRAS, DONALD J.; WASSERBURG, G. J.;. (1980). Neodymium isotopic variations in seawater. *Earth and Planetary Science Letters, 50*, 128-138.

RAHMSTORF, S. (2002, September 12). Ocean circulation and climate during the past 120 000 years. *Nature, 419*, 207-214.

RAHMSTORF, S. (2006). Thermohaline Ocean Circulation. (S. A. Elias, Ed.) *Encyclopedia of Quaternary Sciences*.

REYNOLDS, B. C., FRANK, M., & O'NIONS, R. K. (1999). Nd- and Pb-isotope time series from Atlantic ferromanganese crusts: implications for changes in provenance and paleocirculation over the last 8 Myr. *Earth and Planetary Science Letters, 173*, 381-396.

ROBERTS, N. L., PIOTROWSKI, A. M., MCMANUS, J. F., & KEIGWIN, L. D. (2010). Synchronous deglacial overturning and water mass source changes. Science, 327(5961), 75-78.

STEIN , R., HEFTER, J., GRÜTZNER, J., VOELKER, A., & NAAFS, B. A. (2009). Variability of surface water characteristics and Heinrich-like events in the Pleistocene midlatitude North Atlanticc Ocean: Biomarker and XRD records from IODP Site U1313 (MIS 16-9). *Paleoceanography, 24*.

TACHIKAWA, K., JEANDEL, C., & ROY-BARMAN, M. (1999). A new approach to the Nd residence time in the ocean: The role of atmospheric inputs. *Earth Planet Science Letters, 170*, 433-446.

TANAKA, T., TOGASHI, S., KAMIOKA, H., AMAKAWA, H., KAGAMI, H., HAMAMOTO, T., et al. (2000). JNdi-1: a neodymium isotopic reference in consistency with La Jolla neodymium. *Chemical Geology, 168 (3-4)*, 279-281.

VANCE, D., & THIRLWALL, M. (2002). An assessment of mass discrimination in MC-ICPMS using Nd isotopes. *Chemical Geology, 185*, 227-240.

WEFER, G., BIJMA, J., G., F., & BERGER, W. H. (1999). Clues to Ocean History: A Brief Overview of Proxies. In G. Fischer, & G. Wefer, *THE USE OF PROXIES IN PALEOCEANOGRAPHY, Exemples from the South Atlantic* (pp. 1-68). Berlin: Springer.

ANNEX A

Nd & Sr processing compiled and tested by Evelyn Böhm and Patrick Blaser, Institute for Environmental Physics, University of Heidelberg, Germany

Step 1: Weighing

Weighing the samples into tubes: 0.2 – 0.3 g

Step 2: Dissolution of Carbonates

Chemicals: (per sample)
- 8 ml Na-Acetate buffer solution (pH = 4.66)

Procedure:
- fill tube with 5 ml buffer
- shake a while
- open tube to release gas
- add another 3 ml of buffer
- shake
- put on shaker for 2-3 h

(depending on carbonate content some samples will take (much) longer than that)

- open tube to release gas
- centrifuge: 4 min, 2400 rpm
- decant the liquid (and throw away)

(maybe the dissolved carbonate should be treated and analyzed aswell → keep it!)

Step 3: Removal of Adsorbed Metals

Chemicals: (per sample)
- 5 ml 1M $MgCl_2$ solution
- 24 ml Milli-Q water

Procedure:
- fill tube with 5 ml of $MgCl_2$ solution

- shake and beat until sediment is completely loose
- put on shaker for 1 h
- centrifuge: 5 min, 2000 rpm
- decant and throw away the liquid

- add 12 ml Milli-Q
- shake and beat
- centrifuge: 5 min, 2000 rpm
- decant and throw away the liquid

- add 12 ml Milli-Q
- shake and beat
- centrifuge: 5 min, 2000 rpm
- decant and throw away the liquid

<u>Step 4</u>: Leaching of Fe-Mn-Hydroxide Coatings

Chemicals: - 8.5 ml Nd-leach
(per sample) - 24 ml Milli-Q
- PP-beaker

Procedure: - fill 8.5 ml Nd-leach into tubes
- shake and beat until sediment is completely loose
- put on shaker for (exactly) 2 h
- shake
- centrifuge: 10 min, 4000 rpm
- decant 6 ml of leachate into PP-beaker (no sediment must be pipetted)
- throw away remaining liquid
(*harmful for the environment* → collect in bottle)

For 24 h leach repeat leaching procedure with the samples resting ± 24 h on the shaker.

- fill 12 ml Milli-Q into tube

- shake and beat
- centrifuge: 5 min, 2000 rpm
- decant and throw away the liquid

- fill 12 ml Milli-Q into tube
- shake and beat
- centrifuge: 5 min, 2000 rpm
- decant and throw away the liquid

- store tube or transfer samples into microwave beakers with HCl_{conc} for total digestion

<u>Step 5</u>: Convert into Chloride Form

Chemicals: - 1 ml $HNO_{3,conc}$
(per sample) - 2 ml 9M HCl
- 2 ml 1M HCl
- H_2O_2

Procedure: - dry samples in PP-beakers under infrared lamps
- dissolve in ~ 1 ml $HNO_{3,conc}$ (**WARNING**: gassing!)
- dry under infrared lamps
- dissolve in ~ 1 - 2 ml 9M HCl and add some drops of H_2O_2 (**WARNING**: gassing!)
- dry under infrared lamps
- dissolve in 2 ml 1M HCl

<u>Step 6</u>: 1st column for separation of REE

Chemicals: - 23.5 ml 6M HCl
(per sample) - 3 ml 1M HCl
- 15 ml 2.5M HCl

- 15 ml Milli-Q
- 2.5 ml Dowex 50 WX 8 (200-400µm mesh)
- 2 x PP-beaker
- 12 ml PP BioRad columns

Procedure:
- fill columns with 2.5 ml Dowex 50 WX 8
- clean columns with 1 CV Milli-Q
- clean with 16 ml (~2 CV) 6M HCl
- clean with 2 ml Milli-Q
- load column with 2 x 1.5 ml 1M HCl

- pour sample on column
- rinse column with 3 x 250 µl 2.5M HCl
- rinse with 4 ml 2.5M HCl
- place **Sr-beaker** under column
- eluate Sr with 10 ml (~1 CV) 2.5M HCl
- place **Nd-beaker** under column
- eluate first with 2 x 250 µl and then 7.5 ml 6M HCl

Step 7: Convert to Nitrate Form

Chemicals (per sample):
- 1.2 ml 0.05M HNO_3*

Procedure:
- dry samples in PP-beakers under infrared lamps
- dissolve sample in 1.2 ml 0.05M HNO_3*

Step 8: 2nd column for separation of Nd

Chemicals (per sample):
- recycle-column (5 ml Pipette, frit, 3 cm LN-Resin mesh 100-150 µm)
- 26 ml 0.05M HNO_3*
- 1 ml 1M HNO_3
- 13.5 ml 0.2M HCl*

- 10 ml 6M HCl
- 5 ml 0.2M HCl (uncalibrated)
- 1 ml 1M HCl
- PP-beaker

Procedure: - if necessary, build the recycle-column by cutting off the top and the tip of a 5ml pipette, push in the frit, fill 3 cm high with LN-Resin, wet with 0.05M HNO_3* and flip and ultrasonicate to get rid of all air bubbles

- clean columns with 4 ml 0.05M HNO_3*
- precondition with 1 ml 1M HNO_3
- load column with 2 x 1 ml 0.05M HNO_3*
- load with 10 ml 0.05M HNO_3*

- pour sample on column
- rinse with 4 x 250 µl 0.2M HCl*
- rinse with 4.5 ml and then 4 ml 0.2M HCl*
- place **Nd-sample beaker** under column
- eluate sample with 4 ml 0.2M HCl*

(might be good to eluate with 5 or 6 ml to get more Nd)

- remove sample-beaker

- clean columns with 5 ml + 1 CV 6M HCl
- clean with 5 ml 0.2M HCl (uncalibrated)
- fill column with 1 ml 1M HCl and place upright in box filled with 1M HCl for storing

<u>Step 9</u>: Conversion for Measurement

Chemicals: - 1.5 ml 0.05M HNO_3
(per sample)

Procedure: - dry samples in PP-beakers under infrared lamps
- dissolve sample in 1.5 ml 0.05M HNO_3
- filter, dilute if necessary, and transfer in adequate tube for measurement

The leaching process follows Gutjahr *et al.* 2007

Nd-leach solution:

Titriplex (372.24 g/mol):	10.08 g/l
Hydroxylamine-Hydrochloride (69.49 g/mol):	3.4745 g/l
Acetic Acid (15 %):	150.16 ml/l
Milli-Q	848.757 ml/l

→ add NaOH until solution is buffered at pH = 4

The 2nd Nd-column is modified after Pin *et al.* 1994 and www.eichrom.com/radiochem/meetings/2002/paris/A_practical_guide_to_Sr_Nd_Sm_elemental.pdf

The necessary frits are from Roland Vetter (PE, diameter 3.2 mm, thickness 3 mm, 40 – 100 µm pores)
The columns can be recycled up to 10 times.

ANNEX B

Table of data from the studies used in comparison, references: Gutjahr and Lippold (2012); Roberts et al (2010); Gutjahr et al (2008):

core	ODP1063			ODP1063			12JPC		
author	Gutjahr and Lippold 2011			Roberts et al. 2010			Gutjahr et al. 2008		
lat N	33.700			33.700			29.000		
long W	57.610			57.610			72.500		
depth (m)	4584			4584			4250		
	age [ka]	eNd	err absolute	age [ka]	eNd	err absolute	age [ka]	eNd	err absolute
	15.23	-10.75	0.87	0.29	-12.74	0.89	2.55	-13.40	0.67
	15.56	-10.63	0.74	0.29	-13.83	0.58	3.82	-12.80	0.64
	15.88	-10.69	0.69	0.29	-13.83	0.39	5.09	-13.90	0.70
	16.07	-10.56	0.64	0.29	-13.63	0.84	7.66	-13.30	0.67
	16.23	-10.71	0.30	1.64	-14.9	0.34	8.94	-14.30	0.72
	16.33	-11.35	0.30	4.92	-14.58	0.58	11.00	-14.00	0.70
	16.47	-10.92	0.30	5.89	-14.78	0.34	11.49	-13.50	0.68
	16.60	-11.56	0.30	8.53	-16.15	0.45	11.90	-12.60	0.63
	16.73	-11.19	0.30	8.53	-16.06	0.39	12.14	-12.40	0.62
	16.86	-11.69	0.30	8.53	-16.2	0.32	12.74	-12.00	0.60
	17.00	-11.19	0.30	11.5	-14.63	0.39	14.02	-10.80	0.54
	17.13	-11.31	0.30	11.5	-14.38	0.39	14.56	-10.30	0.52
	17.26	-11.31	0.30	11.5	-14.58	0.48	15.39	-10.70	0.54
	17.39	-11.41	0.30	12.05	-12.59	0.39	15.96	-9.60	0.48
	17.52	-11.29	0.50	12.05	-12.91	0.45	16.54	-10.00	0.50
	17.66	-12.22	0.61	12.43	-11.73	0.58	17.29	-10.40	0.52
	17.89	-11.34	0.30	12.43	-12.06	0.72	17.65	-9.90	0.50
	18.17	-11.36	0.30	12.43	-12.26	0.32	18.26	-10.00	0.50
	18.44	-10.88	0.61	12.83	-13.31	0.45	18.73	-10.30	0.52
	19.27	-11.38	0.59	12.83	-13.26	0.45	19.41	-10.30	0.52
	20.10	-11.61	0.47	13.22	-13.17	0.58	19.87	-10.80	0.54
	20.90	-11.52	0.30	13.22	-12.4	0.58			
	21.73	-10.99	0.39	13.22	-13.58	0.41			
	22.56	-11.83	0.30	14.3	-13.61	0.45			
	23.40	-12.23	0.30	14.3	-13.57	0.45			
	23.86	-12.52	0.57	14.3	-13.97	0.49			
				14.61	-10.86	0.45			
				14.61	-10.82	0.32			
				14.99	-11.13	0.39			
				15.31	-10.82	0.39			
				15.31	-11.65	0.32			
				16.21	-10.68	0.39			
				16.21	-10.48	0.32			
				16.68	-10.61	0.39			
				17.41	-11.23	0.45			
				17.69	-10.33	0.45			
				17.69	-10.87	0.32			
				18.52	-10.71	0.39			
				19.22	-10.66	0.45			
				19.22	-10.55	0.32			
				19.81	-10.35	0.45			
				19.81	-10.76	0.31			

ANNEX C

Chart of data record extracted from Roberts et al (2010), data used to comparisons in chapter "Results and
Discussions"

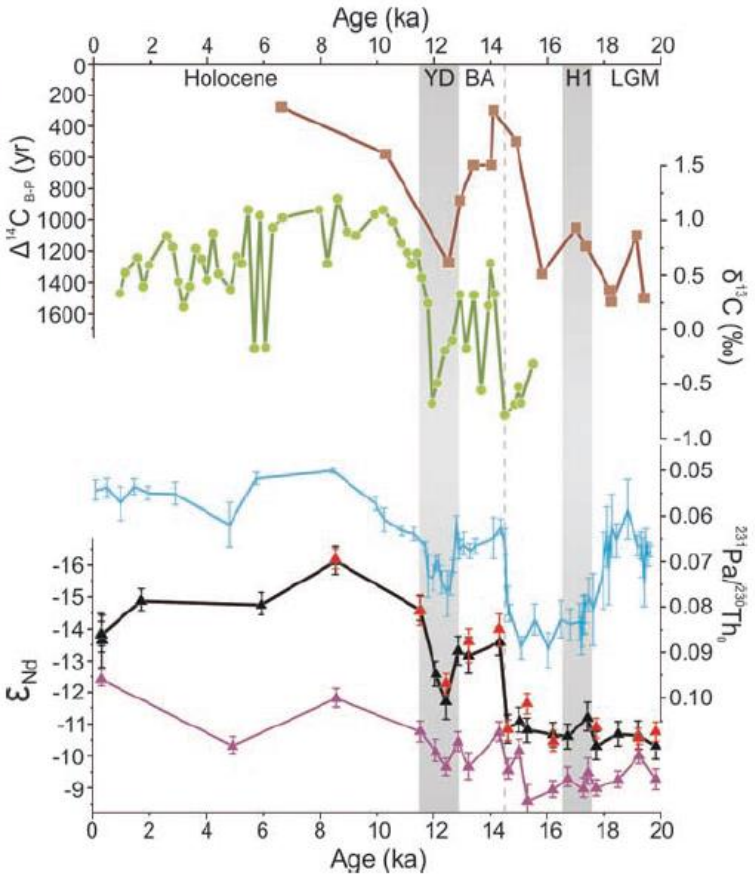

Fig. 3. GGC6 sediment leachates (purple triangles), unclean foraminifera (black triangles), and reductively cleaned fish debris (red triangles), plotted with GGC5 $^{231}Pa/^{230}Th_0$ ratios (blue line) (*22*), GGC1 benthic $\delta^{13}C$ (green circles) [(*19*); for age model see (*9*)], and $\Delta^{14}C$ paired benthic and planktonic apparent ventilation ages (brown squares) (*25*, *26*). The Holocene, Younger Dryas (YD), Bølling-Allerød (BA), Heinrich event 1 (H1), and 14,600 years ago (gray dashed line) are indicated; ka, thousands of years ago. Modern NADW ε_{Nd} ~ –14 and AABW ε_{Nd} ~ –7 to –9 (*4*, *5*, *7*).

ANNEX D

Chart of data record extracted from Gutjahr et al (2008), data used to comparisons in chapter "Results and Discussions"

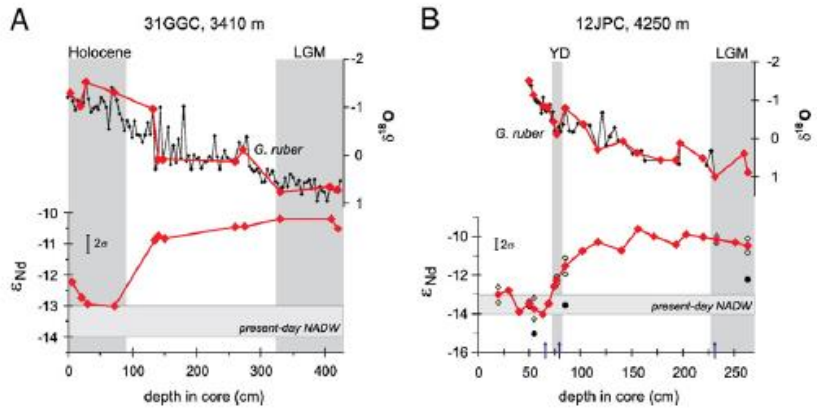

Fig. 4. Downcore seawater Nd isotope results from this study and $\delta^{18}O$ stratigraphy from Keigwin (2004) (sampled depths in $\delta^{18}O$ plot are marked by red dots) for (A) core 31GGC in 3410 m and (B) 12JPC in 4250 m water depth along the deeper Blake Ridge. Average results are plotted for depths in core for which duplicate analyses were carried out, however individual results are also shown (yellow filled diamonds). Black circles represent Nd isotope compositions of the detrital fraction. The modern NADW ε_{Nd}, as measured by Piepgras and Wasserburg (1987), is shown in grey box. Typical interglacial LNADW signatures were only recorded after the YD. Individual Nd isotope data are presented in Tables 1 and 5. Blue arrows in B indicate absolute age tie points published in Keigwin (2004) and Robinson et al. (2005). (For interpretation of the references to colour in this figure legend, the reader is referred to the web version of this article.)

ANNEX E

ANNEX A - Chart of data record extracted from Gutjahr and Lippold (2011), data used to comparisons in chapter “Results and Discussions”

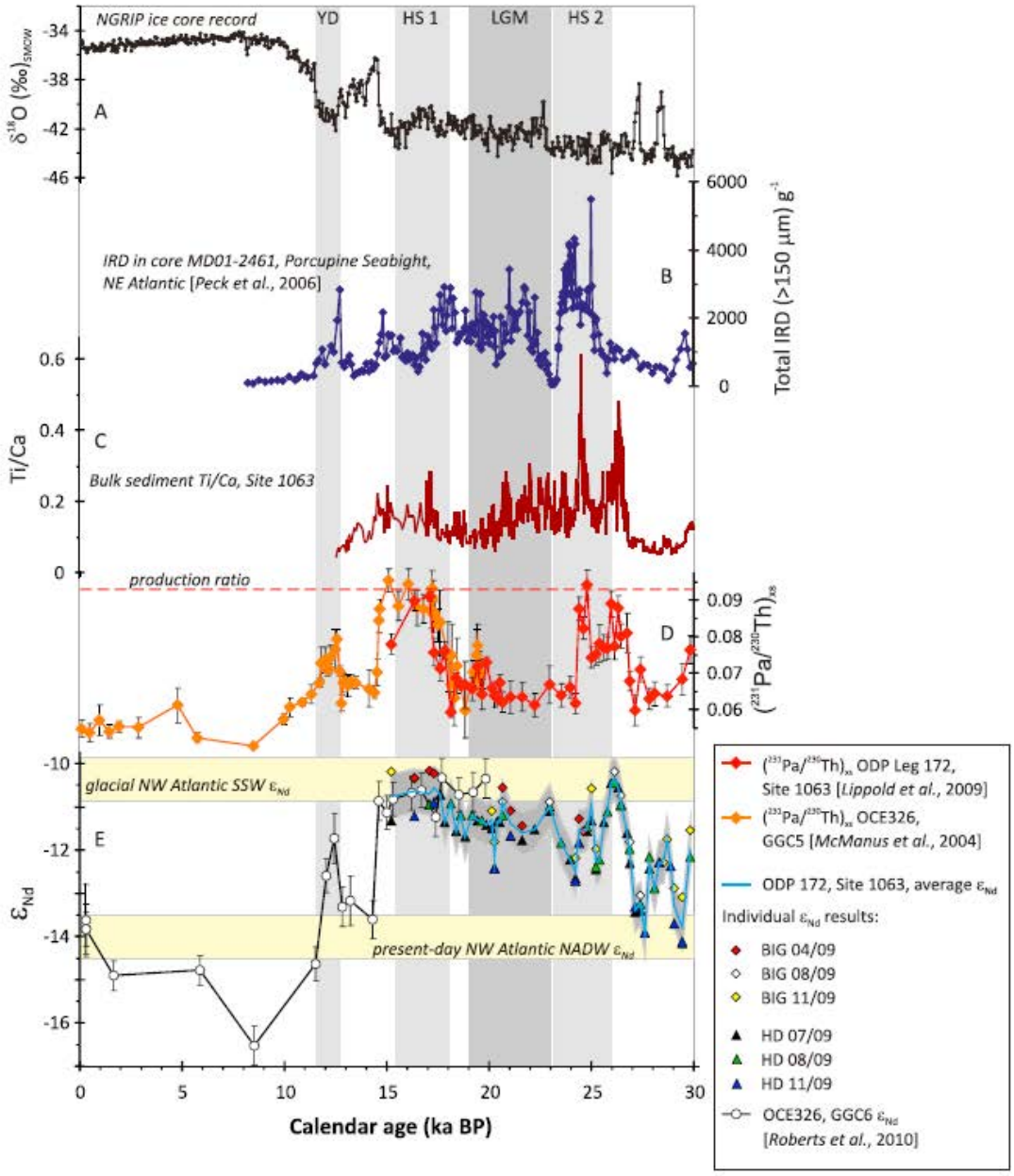

Figure 1. (e) Bermuda Rise bottom water $^{143}Nd/^{144}Nd$ isotope record covering the past 30 kyr, expressed in the ε_{Nd} notation, representing the $^{143}Nd/^{144}Nd$ deviation of a sample relative to chondrite uniform reservoir in parts per 10,000. The new ε_{Nd} data are presented together with and overlap those of *Roberts et al.* [2010], which extend from the latest LGM to the present-day and that were obtained by leaching of uncleaned foraminifera instead of bulk sediments. A large number of duplicates were produced in the course of our study and all data points are shown. The average Nd isotope composition for each sampled sedimentary depth including a gray 0.5 ε_{Nd} error envelope is also shown for better visibility of the patterns. The horizontal yellow boxes in the Figure 1e indicate modern NADW ε_{Nd} as well as deep northwest Atlantic SSW ε_{Nd} during the LGM ($\varepsilon_{Nd} = -10.3 \pm 0.5$) [*Gutjahr et al.*, 2008; *Roberts et al.*, 2010]. (c) Bulk sediment Ti/Ca [*Lippold et al.*, 2009] and (b) NE Atlantic IRD records from the Porcupine Seabight [*Peck et al.*, 2006] are shown for comparison. (d) Pa/Th data are from ODP Site 1063 [*Lippold et al.*, 2009] and OCE326 GGC5 [*McManus et al.*, 2004]. (a) NGRIP ice core oxygen isotope record [*North Greenland Ice Core Project Members*, 2004]. Timing and duration of Heinrich Stadials 1 and 2 were adopted from *Bard et al.* [2000] and *Barker et al.* [2009].